

Isobar model for kaon photoproduction with spin-7/2 and -9/2 nucleon resonances

S. Clymton and T. Mart*

Departemen Fisika, FMIPA, Universitas Indonesia, Depok 16424, Indonesia

(Received 16 August 2016; revised manuscript received 28 February 2017; published 5 September 2017)

We have investigated the effects of spin-7/2 and -9/2 nucleon resonances in the kaon photoproduction process $\gamma p \rightarrow K^+\Lambda$. To this end, the corresponding propagators were derived from the generalized spin projection operators. To remove the lower spin backgrounds in the scattering amplitude, we used the vertex factors obtained from the consistent interaction Lagrangians inspired by Pascalutsa and Vrancx *et al.* The scattering amplitude was included in our previous isobar model, and the effects of four nucleon resonances with spins 7/2 and 9/2 listed by the Particle Data Group were investigated by making use of all available kaon photoproduction data. A significant improvement to our previous model has been observed in all observables, especially in the beam-recoil double-polarization observables C_x , C_z , $O_{x'}$, and $O_{z'}$.

DOI: 10.1103/PhysRevD.96.054004

I. INTRODUCTION

Recently, we have investigated the effect of different formulations of spin-3/2 and -5/2 nucleon resonances on a phenomenological model of an elementary kaon photoproduction process [1]. For this purpose we used an isobar model, where the scattering amplitude is formulated by using the field theoretical approach. The background part of the model was constructed from the standard s -, u -, and t -channel Born amplitudes along with the K^{*+} (892), K_1 (1270), Λ^* (1600), and Λ^* (1810) states. The resonance part used all nucleon resonances listed by the Particle Data Group (PDG) [2] with spins up to 5/2 and with at least a two-star rating. Two different interaction Lagrangians of spin-3/2 and -5/2 nucleon resonances, i.e., the standard formulation given in Refs. [3,4] and the consistent interaction proposed by Pascalutsa [5], were compared. By fitting the calculated observables to nearly 7400 experimental data points, it was found that the use of consistent interaction formulation for the spin-3/2 and -5/2 resonances in the model leads to a better agreement with experimental data.

In spite of this success, however, there exist four nucleon resonances with spins 7/2 and 9/2 listed by PDG [2] (see Table I), where three of them have a four-star rating. Since their statuses are mostly certain and, as such, they fulfill the criteria of resonances used in our model [1], we believe that the inclusion of these resonances in our model is mandatory.

To our knowledge, in the kaon photoproduction and electroproduction studies, the inclusion of nucleon resonances with spins higher than 5/2 in the framework of the field theoretical approach was never considered before. The reason is also obvious: unless we used the multipoles approach [6], the formulation of propagator and vertex

factors of higher spin resonances is quite complicated, not unique, and plagued with the problem of lower spin backgrounds [5,7–9].

Therefore, it is the aim of this paper to present the amplitudes of spin-7/2 and -9/2 nucleon resonances and investigate their effects on the isobar model of kaon photoproduction. For the sake of completeness and future studies, we will derive the formalism for electroproduction, instead of photoproduction, since the latter can be obtained by setting the longitudinal terms k^2 and $k \cdot \epsilon$ to zero.

This paper is organized as follows. In Sec. II we present the formalism of spin-7/2 and -9/2 used in our investigation. In Sec. III we present and discuss the result of our calculation and compare it with the result of previous calculations along with the available experimental data. We will summarize and conclude our findings in Sec. IV.

II. FORMALISM

A. The consistent interaction theory

In what follows, we adopt the prescriptions of Pascalutsa [10,11] and Vrancx *et al.* [7]. We begin with the gauge-invariant field $G_{\mu\nu}$ [10] and the interaction operator $O_{(\mu\nu)\lambda}^{3/2}$ [7] to construct the consistent interaction Lagrangian for massive spin-3/2 particles, where

TABLE I. The status, mass, and width of nucleon resonances with spins 7/2 and 9/2 used in our calculation [2].

Resonance	$L_{21,2J}$	J^P	Status	Mass (MeV)	Width (MeV)
$N(1990)$	F_{17}	$7/2^+$	**	1990 ± 120	240 ± 50
$N(2190)$	G_{17}	$7/2^-$	****	2190^{+10}_{-90}	500 ± 200
$N(2220)$	H_{19}	$9/2^+$	****	2250 ± 50	400^{+100}_{-50}
$N(2250)$	G_{19}	$9/2^-$	****	2275 ± 75	500^{+300}_{-270}

* terry.mart@sci.ui.ac.id

$$\begin{aligned}
G_{\mu\nu} &= \partial_\mu \psi_\nu - \partial_\nu \psi_\mu \\
&= (\partial_\mu g_{\nu\lambda} - \partial_\nu g_{\mu\lambda}) \psi^\lambda \\
&= O_{(\mu,\nu)\lambda}^{3/2} \psi^\lambda,
\end{aligned} \tag{1}$$

with

$$O_{(\mu,\nu)\lambda}^{3/2} = \partial_\mu g_{\nu\lambda} - \partial_\nu g_{\mu\lambda}, \tag{2}$$

and ψ_μ is the massive Rarita-Schwinger (RS) field obeying the RS equation of motion and constraint. In the case of the spin- $(n+1/2)$ particle, the RS equations of motion and constraint read

$$(i\partial - m)\psi_{\mu_1 \dots \mu_n} = 0, \tag{3}$$

$$\gamma^{\mu_1} \psi_{\mu_1 \dots \mu_n} = 0. \tag{4}$$

Since the field $G_{\mu\nu}$ in Eq. (1) contains more indices than the original one, ψ_μ , it is necessary to introduce a new field $\Psi_\mu = O_{(\mu,\nu)\lambda}^{3/2} \gamma^\nu \psi^\lambda$ [7]. As a consequence, in the case of the spin- $(n+1/2)$ particles, the gauge-invariant field reads

$$\Psi_{\mu_1 \dots \mu_n} = O_{(\mu_1 \dots \mu_n, \nu_1 \dots \nu_n) \lambda_1 \dots \lambda_n}^{n+1/2} (\partial) \gamma^{\nu_1} \dots \gamma^{\nu_n} \psi^{\lambda_1 \dots \lambda_n}, \tag{5}$$

with the corresponding interaction operator given by

$$O_{(\mu_1 \dots \mu_n, \nu_1 \dots \nu_n) \lambda_1 \dots \lambda_n}^{n+1/2} (\partial) = \frac{1}{(n!)^2} \sum_{P(\nu)} \sum_{P(\lambda)} O_{(\mu_1, \nu_1) \lambda_1}^{3/2} \dots O_{(\mu_n, \nu_n) \lambda_n}^{3/2}, \tag{6}$$

where $P(\mu)$ and $P(\nu)$ indicate the permutations of all possible μ and ν indices, respectively. Armed with Eqs. (5) and (6) we can construct a consistent interaction Lagrangian for higher spin particles inspired by Pascalutsa's prescription for spin-3/2 particles [11].

The hadronic interaction Lagrangian for the spin-3/2 nucleon resonance N^* decaying to a kaon K and a hyperon Λ shown in Fig. 1 reads [11]

$$\mathcal{L}_{\text{had}} = \frac{g_{K\Lambda N^*}}{m_{N^*}^2} \epsilon^{\mu\nu\alpha\beta} \bar{\Psi} \partial_\beta \phi^* \gamma_5 \gamma_\alpha (\partial_\mu \psi_\nu) + \text{H.c.}, \tag{7}$$

where $\bar{\Psi}$ is the spinor field of Λ , ϕ is the pseudoscalar field of K , and ψ_μ is the massive RS field of N^* . A consistent interaction can be constructed from Eq. (7) by replacing ψ_μ with Ψ_μ/m_{N^*} , i.e.,

$$\mathcal{L}_{\text{had}} = \frac{g_{K\Lambda N^*}}{m_{N^*}^3} \epsilon^{\mu\nu\alpha\beta} \bar{\Psi} \partial_\beta \phi^* \gamma_5 \gamma_\alpha (\partial_\mu \Psi_\nu) + \text{H.c.}, \tag{8}$$

so that in the case of the spin- $(n+1/2)$ nucleon resonance, we obtain

$$\begin{aligned}
\mathcal{L}_{\text{had}} &= \frac{g_{K\Lambda N^*}}{m_{N^*}^{2n+1}} \epsilon^{\mu\nu\alpha\beta} \partial^{\nu_1} \dots \partial^{\nu_{n-1}} \bar{\Psi} \partial_\beta \phi^* \gamma_5 \gamma_\alpha \\
&\quad \times \partial_\mu \Psi_{\nu_1 \dots \nu_n} + \text{H.c.}
\end{aligned} \tag{9}$$

The electromagnetic interaction can be obtained by using the same procedure. Based on Ref. [5] we can write the Lagrangian for the spin-3/2 particle as

$$\begin{aligned}
\mathcal{L}_{\text{em}} &= \frac{e}{m_{N^*}^3} \bar{\Psi}^\beta \{ (g_1 \epsilon_{\mu\nu\alpha\beta} \partial^\alpha \Psi + g_2 \gamma_5 g_{\beta\nu} \partial_\mu \Psi \\
&\quad + g_3 \gamma_\mu \gamma^\rho \epsilon_{\rho\nu\alpha\beta} \partial^\alpha \Psi \\
&\quad + g_4 \gamma_5 \gamma_\mu \gamma^\rho (\partial_\rho g_{\nu\beta} - \partial_\nu g_{\rho\beta}) \Psi \} F^{\mu\nu} + \text{H.c.}
\end{aligned} \tag{10}$$

Therefore, the consistent interaction Lagrangian for the spin- $(n+1/2)$ nucleon resonance reads

$$\begin{aligned}
\mathcal{L}_{\text{em}} &= \frac{e}{m_{N^*}^{2n+1}} \bar{\Psi}^{\beta_1 \dots \beta_n} \{ (g_1 \epsilon_{\mu\nu\alpha\beta_n} \partial^\alpha \Psi + g_2 \gamma_5 g_{\beta_n\nu} \partial_\mu \Psi \\
&\quad + g_3 \gamma_\mu \gamma^\rho \epsilon_{\rho\nu\alpha\beta_n} \partial^\alpha \Psi \\
&\quad + g_4 \gamma_5 \gamma_\mu \gamma^\rho (\partial_\rho g_{\nu\beta_n} - \partial_\nu g_{\rho\beta_n}) \Psi \} \partial_{\beta_1} \dots \partial_{\beta_{n-1}} F^{\mu\nu} \\
&\quad + \text{H.c.}
\end{aligned} \tag{11}$$

The above-mentioned interaction is consistent because it contains the interaction operator which fulfills

$$p_{N^*}^{\lambda_i} O_{(\mu_1 \dots \mu_n, \nu_1 \dots \nu_n) \lambda_1 \dots \lambda_n}^{n+1/2} (p_{N^*}) = 0, \tag{12}$$

where $i = 1, 2, \dots, n$ and $p_{N^*}^{\lambda_i}$ is the four-momentum of the spin- $(n+1/2)$ nucleon resonance (see Fig. 1).

With the definition of particle momenta and coupling strengths given in Fig. 1, the hadronic and electromagnetic vertex factors derived from Eqs. (9) and (11) can be written as

$$\begin{aligned}
\Gamma_{\mu_1 \dots \mu_n}^{\text{had}} &= \frac{g_{K\Lambda N^*}}{m_{N^*}^{2n+1}} \epsilon^{\mu\nu\alpha\beta} p_\Lambda^{\nu_1} \dots p_\Lambda^{\nu_{n-1}} q_\beta \gamma_5 \gamma_\alpha p_{N^*}^\mu \\
&\quad \times O_{(\nu_1 \dots \nu_n, \alpha_1 \dots \alpha_n) \mu_1 \dots \mu_n}^{n+1/2} (p_{N^*}) \gamma^{\alpha_1} \dots \gamma^{\alpha_n}
\end{aligned} \tag{13}$$

and

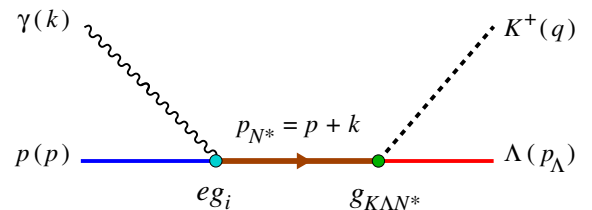


FIG. 1. Feynman diagram for the nucleon resonance (N^*) intermediate state in the kaon photoproduction $\gamma p \rightarrow K^+ \Lambda$.

$$\Gamma_{\nu_1 \cdots \nu_n}^{\text{em}} = \frac{e}{m_{N^*}^{2n+1}} \mathcal{O}_{n+1/2}^{(\beta_1 \cdots \beta_n, \alpha_1 \cdots \alpha_n) \nu_1 \cdots \nu_n} (p_{N^*}) \gamma_{\alpha_1} \cdots \gamma_{\alpha_n} \{g_1 \epsilon_{\mu\nu\alpha\beta_n} P^\alpha + g_2 \gamma_5 g_{\beta_n \nu} P_\mu + g_3 \gamma_\mu \gamma^\rho \epsilon_{\rho\nu\alpha\beta_n} P^\alpha + g_4 \gamma_5 \gamma_\mu \gamma^\rho (P_\rho g_{\nu\beta_n} - P_\nu g_{\rho\beta_n})\} k_{\beta_1} \cdots k_{\beta_{n-1}} (k^\mu \epsilon^\nu - k^\nu \epsilon^\mu), \quad (14)$$

which can be written in more compact forms, i.e.,

$$\Gamma_{\mu_1 \cdots \mu_n}^{\text{had}} = \frac{1}{m_{N^*}^n} \tilde{\Gamma}_{\text{had}}^{\nu_1 \cdots \nu_n} \tilde{\mathcal{O}}_{(\nu_1 \cdots \nu_n) \mu_1 \cdots \mu_n}^{n+1/2} (p_{N^*}) \quad (15)$$

and

$$\Gamma_{\mu_1 \cdots \mu_n}^{\text{em}} = \frac{1}{m_{N^*}^n} \tilde{\mathcal{O}}_{(\nu_1 \cdots \nu_n) \mu_1 \cdots \mu_n}^{n+1/2} (p_{N^*}) \tilde{\Gamma}_{\text{em}}^{\nu_1 \cdots \nu_n}, \quad (16)$$

with

$$\tilde{\mathcal{O}}_{(\nu_1 \cdots \nu_n) \mu_1 \cdots \mu_n}^{n+1/2} (p_{N^*}) = \mathcal{O}_{(\nu_1 \cdots \nu_n, \alpha_1 \cdots \alpha_n) \mu_1 \cdots \mu_n}^{n+1/2} (p_{N^*}) \gamma^{\alpha_1} \cdots \gamma^{\alpha_n}. \quad (17)$$

The contribution of the spin- $(n+1/2)$ nucleon resonance to the production amplitude that is relevant to the present investigation has the following structure:

$$\mathcal{M}_{N^*}^{n+1/2} = \bar{u}_\Lambda \Gamma_{\mu_1 \cdots \mu_n}^{\text{had}} P_{(n+1/2)}^{\mu_1 \cdots \mu_n, \nu_1 \cdots \nu_n} (p_{N^*}) \Gamma_{\nu_1 \cdots \nu_n}^{\text{em}} u_p, \quad (18)$$

where $P_{(n+1/2)}^{\mu_1 \cdots \mu_n, \nu_1 \cdots \nu_n}$ is the spin- $(n+1/2)$ nucleon resonance propagator. For the purpose of the present discussion we can utilize the propagator discussed by Vrancx *et al.* [7] which is based on the work of Huang *et al.* [12]. We shall use the covariant part of the propagator, since the non-covariant one does not preserve the Lorentz invariance. Explicitly, it is given by [7]

$$P_{(n+1/2)}^{\mu_1 \cdots \mu_n, \nu_1 \cdots \nu_n} (p_{N^*}) = \frac{\not{p}_{N^*} + m_{N^*}}{p_{N^*}^2 - m_{N^*}^2 + im_{N^*} \Gamma} \tilde{\mathcal{P}}_{(n+1/2)}^{\mu_1 \cdots \mu_n, \nu_1 \cdots \nu_n} (p_{N^*}), \quad (19)$$

where the on-shell projection operator $\tilde{\mathcal{P}}_{(n+1/2)}^{\mu_1 \cdots \mu_n, \nu_1 \cdots \nu_n} (p_{N^*})$ is obtained from the off-shell projection operator $\mathcal{P}_{(n+1/2)}^{\mu_1 \cdots \mu_n, \nu_1 \cdots \nu_n} (p_{N^*})$ with the substitutions $\not{p}_{N^*} \rightarrow m_{N^*}$ and

$p_{N^*}^2 \rightarrow m_{N^*}^2$. We will discuss the explicit form of projection operators for spin-7/2 and -9/2 nucleon resonances later.

It is obvious that the difference between the on-shell projection operator $\tilde{\mathcal{P}}_{(n+1/2)}^{\mu_1 \cdots \mu_n, \nu_1 \cdots \nu_n} (p_{N^*})$ and the off-shell projection operator $\mathcal{P}_{(n+1/2)}^{\mu_1 \cdots \mu_n, \nu_1 \cdots \nu_n} (p_{N^*})$ is in the momentum-dependent terms. In other words, these terms must contain at least one $p_{N^*}^\mu$. However, these terms completely disappear from the production amplitude of Eq. (18) by imposing the property of the interaction operator as given in Eq. (12).

The proof that the on-shell projection operator $\tilde{\mathcal{P}}_{(n+1/2)}^{\mu_1 \cdots \mu_n, \nu_1 \cdots \nu_n} (p)$ can be written as the sum of the off-shell projection operator $\mathcal{P}_{(n+1/2)}^{\mu_1 \cdots \mu_n, \nu_1 \cdots \nu_n} (p)$ and the momentum-dependent terms is straightforward for the spin-3/2 case [see, e.g., Ref. [7], especially Eqs. (18)–(20) and the corresponding explanation therein]. For the general spin- $(n+1/2)$ particle whose mass and momentum are m and p , respectively, the proof is also obvious since the substitution $\not{p} \rightarrow m$ and $p^2 \rightarrow m^2$ in the off-shell projection operator $\mathcal{P}_{(n+1/2)}^{\mu_1 \cdots \mu_n, \nu_1 \cdots \nu_n} (p)$ will only affect its momentum-dependent terms. Thus, the result can be rewritten as the sum of the off-shell projection operator and the momentum-dependent terms. The explicit form of projection operators for spin-7/2 and -9/2 nucleon resonances given in Eqs. (23) and (24), respectively, provides a direct example to this end.

The above discussion has proven that the interaction Lagrangian used in our formalism, which is taken from Ref. [11], is consistent in the sense that the use of this Lagrangian removes the inconsistent lower spin backgrounds of the propagator. The following discussion will show that the use of this interaction also removes the nonlocalities in the production amplitude. By using a slightly different interaction Lagrangian, Vrancx *et al.* [7] have shown this phenomenon in their paper [see Eqs. (60) of Ref. [7]].

By substituting Eqs. (15) and (16) in Eq. (18) we obtain

$$\begin{aligned} \mathcal{M}_{N^*}^{n+1/2} &= \bar{u}_\Lambda \tilde{\Gamma}_{\text{had}}^{\alpha_1 \cdots \alpha_n} \tilde{\mathcal{O}}_{(\alpha_1 \cdots \alpha_n) \mu_1 \cdots \mu_n}^{n+1/2} (p_{N^*}) \frac{1}{m_{N^*}^{2n}} P_{(n+1/2)}^{\mu_1 \cdots \mu_n, \nu_1 \cdots \nu_n} (p_{N^*}) \tilde{\mathcal{O}}_{(\beta_1 \cdots \beta_n) \nu_1 \cdots \nu_n}^{n+1/2} (p_{N^*}) \tilde{\Gamma}_{\text{em}}^{\beta_1 \cdots \beta_n} u_p \\ &= \bar{u}_\Lambda \tilde{\Gamma}_{\text{had}}^{\alpha_1 \cdots \alpha_n} \tilde{\mathcal{O}}_{(\alpha_1 \cdots \alpha_n) \mu_1 \cdots \mu_n}^{n+1/2} (p_{N^*}) \frac{1}{m_{N^*}^{2n}} \frac{\not{p}_{N^*} + m_{N^*}}{p_{N^*}^2 - m_{N^*}^2 + im_{N^*} \Gamma} \mathcal{P}_{(n+1/2)}^{\mu_1 \cdots \mu_n, \nu_1 \cdots \nu_n} (p_{N^*}) \times \tilde{\mathcal{O}}_{(\beta_1 \cdots \beta_n) \nu_1 \cdots \nu_n}^{n+1/2} (p_{N^*}) \tilde{\Gamma}_{\text{em}}^{\beta_1 \cdots \beta_n} u_p. \end{aligned} \quad (20)$$

Equation (20) can be simplified by utilizing the orthogonality of the projection operator, i.e.,

$$\gamma_{\mu_i} \mathcal{P}_{(n+1/2)}^{\mu_1 \cdots \mu_n, \nu_1 \cdots \nu_n} (p_{N^*}) = \mathcal{P}_{(n+1/2)}^{\mu_1 \cdots \mu_n, \nu_1 \cdots \nu_n} (p_{N^*}) \gamma_{\nu_i} = p_{N^* \mu_i} \mathcal{P}_{(n+1/2)}^{\mu_1 \cdots \mu_n, \nu_1 \cdots \nu_n} (p_{N^*}) = p_{N^* \nu_i} \mathcal{P}_{(n+1/2)}^{\mu_1 \cdots \mu_n, \nu_1 \cdots \nu_n} (p_{N^*}) = 0, \quad (21)$$

where $i = 1, 2, \dots, n$.

There are n Dirac matrices in the interaction operator $\tilde{O}_{(\beta_1 \dots \beta_n) \nu_1 \dots \nu_n}^{n+1/2}(p_{N^*})$ on the right-hand side of the propagator in Eq. (20) as obviously shown by Eq. (17). In Eq. (17) these matrices are contracted with the operator $O_{(\beta_1 \dots \beta_n, \alpha_1 \dots \alpha_n) \nu_1 \dots \nu_n}^{n+1/2}(p_{N^*})$, which is built from a product of n interaction operators $O_{(\beta_i, \alpha_i) \nu_i}^{3/2}$. Clearly, these contractions yield the terms containing $p_{N^*} \beta_i \gamma_{\nu_i}$ and $g_{\beta_i \nu_i} \not{p}_{N^*}$. The terms containing at least one γ_{ν_i} vanish due to Eq. (21). Due to the

permutation $P(\alpha)$ in the interaction operator, we obtain $n!$ surviving terms in Eq. (20). By exploiting the symmetry of the projection operator under the exchange of the index ν_i , these surviving terms can be simply written as $\prod_{i=1}^n \not{p}_{N^*} g_{\beta_i \nu_i}$. The same procedure can also be performed for the interaction operator $\tilde{O}_{(\alpha_1 \dots \alpha_n) \mu_1 \dots \mu_n}^{n+1/2}(p_{N^*})$ on the left-hand side of the propagator in Eq. (20). Therefore, the production amplitude given by Eq. (20) can be written as

$$\begin{aligned} \mathcal{M}_{N^*} &= \bar{u}_\Lambda \prod_{i=1}^n \not{p}_{N^*} g_{\alpha_i \mu_i} \tilde{\Gamma}_{\text{had}}^{\alpha_1 \dots \alpha_n} \frac{1}{m_{N^*}^{2n} p_{N^*}^2 - m_{N^*}^2 + im_{N^*} \Gamma} \not{p}_{N^*} + m_{N^*} \mathcal{P}_{(n+1/2)}^{\mu_1 \dots \mu_n, \nu_1 \dots \nu_n}(p_{N^*}) \prod_{j=1}^n \not{p}_{N^*} g_{\beta_j \nu_j} \tilde{\Gamma}_{\text{em}}^{\beta_1 \dots \beta_n} u_p \\ &= \bar{u}_\Lambda \tilde{\Gamma}_{\mu_1 \dots \mu_n}^{\text{had}} \frac{p_{N^*}^{2n}}{m_{N^*}^{2n} p_{N^*}^2 - m_{N^*}^2 + im_{N^*} \Gamma} \not{p}_{N^*} + m_{N^*} \mathcal{P}_{(n+1/2)}^{\mu_1 \dots \mu_n, \nu_1 \dots \nu_n}(p_{N^*}) \tilde{\Gamma}_{\nu_1 \dots \nu_n}^{\text{em}} u_p. \end{aligned} \quad (22)$$

Equation (22) shows that the nonlocalities in the amplitude are completely removed by the $p_{N^*}^{2n}$ factor. This is equivalent to Eq. (60) of Ref. [7].

B. Spin-7/2 and -9/2 projection operators

The projection operators for spin-7/2 and -9/2 nucleon resonances which are suitable to our previous discussion can be obtained from the generalized higher spin projection operators given in, e.g., Ref. [12]. For the spin-7/2 nucleon resonance the projection operator reads

$$\begin{aligned} \mathcal{P}_{\mu_1 \mu_2 \mu_3 \nu_1 \nu_2 \nu_3}^{7/2} &= \frac{1}{36} \sum_{P(\mu), P(\nu)} \left\{ P_{\mu_1 \nu_1} P_{\mu_2 \nu_2} P_{\mu_3 \nu_3} - \frac{3}{7} P_{\mu_1 \mu_2} P_{\nu_1 \nu_2} P_{\mu_3 \nu_3} \right. \\ &\quad + \frac{3}{7} \gamma^\rho \gamma^\sigma P_{\mu_1 \rho} P_{\nu_1 \sigma} P_{\mu_2 \nu_2} P_{\mu_3 \nu_3} \\ &\quad \left. - \frac{3}{35} \gamma^\rho \gamma^\sigma P_{\mu_1 \rho} P_{\nu_1 \sigma} P_{\mu_2 \mu_3} P_{\nu_2 \nu_3} \right\}, \end{aligned} \quad (23)$$

where $P(\mu)$ and $P(\nu)$ indicate the permutations of all possible μ and ν indices, respectively, while $P_{\mu\nu} = -g_{\mu\nu} + p_{N^*} \mu p_{N^*} \nu / s$ and $p_{N^*} = p + k$. In the case of spin-9/2 nucleon resonance the projection operator reads

$$\begin{aligned} \mathcal{P}_{\mu_1 \mu_2 \mu_3 \mu_4 \nu_1 \nu_2 \nu_3 \nu_4}^{9/2} &= \frac{1}{576} \sum_{P(\mu), P(\nu)} \left\{ P_{\mu_1 \nu_1} P_{\mu_2 \nu_2} P_{\mu_3 \nu_3} P_{\mu_4 \nu_4} \right. \\ &\quad - \frac{6}{9} P_{\mu_1 \mu_2} P_{\nu_1 \nu_2} P_{\mu_3 \nu_3} P_{\mu_4 \nu_4} \\ &\quad + \frac{4}{9} \gamma^\rho \gamma^\sigma P_{\mu_1 \rho} P_{\nu_1 \sigma} P_{\mu_2 \nu_2} P_{\mu_3 \nu_3} P_{\mu_4 \nu_4} \\ &\quad - \frac{4}{21} \gamma^\rho \gamma^\sigma P_{\mu_1 \rho} P_{\nu_1 \sigma} P_{\mu_2 \mu_3} P_{\nu_2 \nu_3} P_{\mu_4 \nu_4} \\ &\quad \left. + \frac{1}{21} P_{\mu_1 \mu_2} P_{\nu_1 \nu_2} P_{\mu_3 \mu_4} P_{\nu_3 \nu_4} \right\}. \end{aligned} \quad (24)$$

Both projection operators given by Eqs. (23) and (24) satisfy the orthogonality condition with respect to the Dirac matrix and the total momentum of the particle, i.e.,

$$\gamma^{\mu_i} \mathcal{P}_{\mu_1 \mu_2 \dots \mu_n \nu_1 \nu_2 \dots \nu_n}^{(n+1/2)} = \mathcal{P}_{\mu_1 \mu_2 \dots \mu_n \nu_1 \nu_2 \dots \nu_n}^{(n+1/2)} \gamma^{\nu_i} = 0 \quad (25)$$

and

$$(p+k)^{\mu_i} \mathcal{P}_{\mu_1 \mu_2 \dots \mu_n \nu_1 \nu_2 \dots \nu_n}^{(n+1/2)} = \mathcal{P}_{\mu_1 \mu_2 \dots \mu_n \nu_1 \nu_2 \dots \nu_n}^{(n+1/2)} (p+k)^{\nu_i} = 0, \quad (26)$$

where $i = 1, 2, \dots, n$. Based on Eq. (22) we can write the modified propagator for the spin-7/2 nucleon resonance as

$$\mathcal{P}_{\mu_1 \mu_2 \nu_1 \nu_2}^{7/2} = \frac{s^3}{m_{N^*}^6 (s - m_{N^*}^2 + im_{N^*} \Gamma_{N^*})} \mathcal{P}_{\mu_1 \mu_2 \nu_1 \nu_2}^{7/2}, \quad (27)$$

where $s = p_{N^*}^2 = (k+p)^2 = W^2$ is one of the Mandelstam variables. In the following, we will also use the other Mandelstam variables $t = (k-q)^2$ and $u = (k-p_\Lambda)^2$.

By using the same procedure, we obtain the modified propagator for spin-9/2 nucleon resonances, i.e.,

$$\mathcal{P}_{\mu_1 \mu_2 \mu_3 \nu_1 \nu_2 \nu_3}^{9/2} = \frac{s^4}{m_{N^*}^8 (s - m_{N^*}^2 + im_{N^*} \Gamma_{N^*})} \mathcal{P}_{\mu_1 \mu_2 \mu_3 \nu_1 \nu_2 \nu_3}^{9/2}. \quad (28)$$

Note that the factors of $s^3/m_{N^*}^6$ and $s^4/m_{N^*}^8$ on the right-hand sides of Eqs. (27) and (28), respectively, appear as a consequence of consistent interaction. In our previous work they were called the regularization factors [1]. These factors are especially important in the case of the u -channel, where the value of the Mandelstam variable u could be zero.

C. Electromagnetic and hadronic vertices

As previously discussed, the electromagnetic and hadronic vertex factors are obtained from an effective

Lagrangian approach proposed by Pascalutsa [5,11], which ensures that the lower spin background of the propagator vanishes [see Eqs. (14) and (13)]. From Eq. (22) it is clear that in calculating the scattering amplitude, we only need $\tilde{\Gamma}_{\mu_1 \dots \mu_n}^{\text{had}}$ and $\tilde{\Gamma}_{\nu_1 \dots \nu_n}^{\text{em}}$, instead of $\Gamma_{\mu_1 \dots \mu_n}^{\text{had}}$ and $\Gamma_{\nu_1 \dots \nu_n}^{\text{em}}$. For the sake of simplicity, in what follows we omit the tilde in both vertex factors. Therefore, the explicit form of the electromagnetic vertex for the spin-7/2 particle reads

$$\begin{aligned} \Gamma_{\text{em}}^{\nu\mu_1\nu_2} &= \frac{k^{\nu_1} k^{\nu_2}}{m_{N^*}^3} [g_{\gamma N^* N}^1 \varepsilon^{\nu\mu\rho\sigma} p_\sigma (k_\mu \varepsilon_\rho - k_\rho \varepsilon_\mu) \\ &\quad + g_{\gamma N^* N}^2 \gamma_5 (p \cdot k \varepsilon^\nu - p \cdot \varepsilon k^\nu) \\ &\quad + g_{\gamma N^* N}^3 \varepsilon^{\nu\mu\rho\sigma} p_\sigma (\not{k} \varepsilon_\mu - \not{\varepsilon} k_\mu) \gamma_\rho \\ &\quad + g_{\gamma N^* N}^4 \gamma_5 \{ (\not{k} \not{p} \varepsilon^\nu - \not{\varepsilon} \not{p} k^\nu) \\ &\quad - (p \cdot \varepsilon \not{k} - p \cdot k \not{\varepsilon}) \gamma^\nu \}, \end{aligned} \quad (29)$$

whereas the hadronic vertex for the spin-7/2 particle is

$$\Gamma_{\text{had}}^{\mu\mu_1\mu_2} = \frac{g_{K\Lambda N^*}}{m_{N^*}^3} i \varepsilon^{\mu\alpha\rho\sigma} p_{\Lambda\alpha} \gamma_5 \gamma_\rho q_\sigma P_\Lambda^{\mu_1} P_\Lambda^{\mu_2}. \quad (30)$$

Note that these vertex factors are constructed for a positive parity intermediate state. In the case of a negative parity intermediate state we can modify these vertices as explained in Ref. [4]. Therefore, we obtain

$$\begin{aligned} \Gamma_{\text{em}}^{\nu\mu_1\nu_2(\pm)} &= \frac{-i}{m_{N^*}^3} [g^1 p^\nu (\not{k} \not{\varepsilon} - \not{\varepsilon} \not{k}) + g^2 (k^\nu p \cdot \varepsilon - \varepsilon^\nu p \cdot k) \\ &\quad + g^3 (\varepsilon^\nu \not{k} - k^\nu \not{\varepsilon}) \not{p} + g^4 \gamma^\nu (\not{k} \not{\varepsilon} - \not{\varepsilon} \not{k}) \not{p} \\ &\quad + g^5 \gamma^\nu (p \cdot \varepsilon \not{k} - p \cdot k \not{\varepsilon})] k^{\nu_1} k^{\nu_2} \Gamma_\pm \end{aligned} \quad (31)$$

and

$$\begin{aligned} \Gamma_{\text{had}}^{\mu\mu_1\mu_2(\pm)} &= \frac{g_{K\Lambda N^*}}{m_{N^*}^3} \Gamma_\mp [(p_\Lambda \cdot q - \not{p}_\Lambda \not{q}) \gamma^\mu + \not{p}_\Lambda q^\mu \\ &\quad - \not{q} P_\Lambda^\mu] P_\Lambda^{\mu_1} P_\Lambda^{\mu_2}, \end{aligned} \quad (32)$$

where

$$\begin{aligned} \mathcal{M}_{7/2}^\pm &= \bar{u}_\Lambda \gamma_5 \{ -s \pm m_{N^*} (\not{p} + \not{k}) \} \left[5(7c_1^2 + c_2c_3) \left\{ -p_{\Lambda\nu} + \frac{1}{s} c_\Lambda (p+k)_\nu \right\} - 10c_1c_2 \left\{ -k_\nu + \frac{1}{s} c_k (p+k)_\nu \right\} \right. \\ &\quad + (5c_1^2 + c_2c_3) \left\{ -\not{p}_\Lambda + \frac{1}{s} c_\Lambda (\not{p} + \not{k}) \right\} \left\{ -\gamma_\nu + \frac{1}{s} (\not{p} + \not{k})(p+k)_\nu \right\} - 10c_1 \left\{ -\not{p}_\Lambda + \frac{1}{s} c_\Lambda (\not{p} + \not{k}) \right\} \\ &\quad \times \left\{ -\not{k} + \frac{1}{s} c_k (\not{p} + \not{k}) \right\} \left\{ -p_{\Lambda\nu} + \frac{1}{s} c_\Lambda (p+k)_\nu \right\} + 2c_2 \left\{ -\not{p}_\Lambda + \frac{1}{s} c_\Lambda (\not{p} + \not{k}) \right\} \left\{ -\not{k} + \frac{1}{s} c_k (\not{p} + \not{k}) \right\} \\ &\quad \times \left\{ -k_\nu + \frac{1}{s} c_k (p+k)_\nu \right\} \left. \right] [G^1 p^\nu (\not{k} \not{\varepsilon} - \not{\varepsilon} \not{k}) + G^2 (k^\nu p \cdot \varepsilon - \varepsilon^\nu p \cdot k) + G^3 (\varepsilon^\nu \not{k} - k^\nu \not{\varepsilon}) \not{p}] u_p, \end{aligned} \quad (36)$$

$$\begin{aligned} g^1 &= ig_{\gamma N^* N}^1 - ig_{\gamma N^* N}^3 \\ g^2 &= -2ig_{\gamma N^* N}^1 - g_{\gamma N^* N}^2 + 2ig_{\gamma N^* N}^3 - 2g_{\gamma N^* N}^4 \\ g^3 &= -2ig_{\gamma N^* N}^1 + 3ig_{\gamma N^* N}^3 + g_{\gamma N^* N}^4 \\ g^4 &= -ig_{\gamma N^* N}^1 + ig_{\gamma N^* N}^3 \\ g^5 &= 2ig_{\gamma N^* N}^1 - ig_{\gamma N^* N}^3 + g_{\gamma N^* N}^4, \end{aligned}$$

with the parity factors $\Gamma_+ = i\gamma_5$ and $\Gamma_- = 1$.

For spin-9/2 particles the vertex factors are obtained by multiplying the vertex factors of spin-7/2 particles with the appropriate momentum and inverting the parity. Thus, the vertex factors of spin-9/2 particles may be written as

$$\begin{aligned} \Gamma_{\text{em}}^{\nu\nu_1\nu_2\nu_3(\pm)} &= \frac{-i}{m_{N^*}^3} [g^1 p^\nu (\not{k} \not{\varepsilon} - \not{\varepsilon} \not{k}) \\ &\quad + g^2 (k^\nu p \cdot \varepsilon - \varepsilon^\nu p \cdot k) + g^3 (\varepsilon^\nu \not{k} - k^\nu \not{\varepsilon}) \not{p} \\ &\quad + g^4 \gamma^\nu (\not{k} \not{\varepsilon} - \not{\varepsilon} \not{k}) \not{p} + g^5 \gamma^\nu (p \cdot \varepsilon \not{k} - p \cdot k \not{\varepsilon})] \\ &\quad \times k^{\nu_1} k^{\nu_2} k^{\nu_3} \Gamma_\mp \end{aligned} \quad (33)$$

and

$$\begin{aligned} \Gamma_{\text{had}}^{\mu\mu_1\mu_2\mu_3(\pm)} &= \frac{g_{K\Lambda N^*}}{m_{N^*}^3} \Gamma_\pm [(p_\Lambda \cdot q - \not{p}_\Lambda \not{q}) \gamma^\mu \\ &\quad + \not{p}_\Lambda q^\mu - \not{q} P_\Lambda^\mu] P_\Lambda^{\mu_1} P_\Lambda^{\mu_2} P_\Lambda^{\mu_3}. \end{aligned} \quad (34)$$

D. Scattering amplitude

The scattering amplitude is obtained by sandwiching the propagator between the hadronic and electromagnetic factors. This was briefly discussed after we introduced Eq. (18). For spin-7/2 nucleon resonances the scattering amplitude becomes

$$\mathcal{M}_{\text{res}}^{7/2} = \bar{u}_\Lambda \Gamma_{K\Lambda N^*}^{\mu\mu_1\mu_2(\pm)} P_{\nu\nu_1\nu_2}^{7/2} \Gamma_{N^* p \gamma}^{\nu\nu_1\nu_2(\pm)} u_p. \quad (35)$$

At first glance, Eq. (35) seems to be very long and complicated. Fortunately, a number of terms in Eq. (35) have the same structure. By exploiting this fact and using the orthogonality condition of projection operators, we can recast the scattering amplitude to

where

$$G^1 = \frac{s^3 g_{K\Lambda N^*} g^1}{35 m_{N^*}^{14} (s - m_{N^*}^2 + i m_{N^*} \Gamma_{N^*})}, \quad (37)$$

$$G^2 = \frac{s^3 g_{K\Lambda N^*} g^2}{35 m_{N^*}^{14} (s - m_{N^*}^2 + i m_{N^*} \Gamma_{N^*})}, \quad (38)$$

$$G^3 = \frac{s^3 g_{K\Lambda N^*} g^3}{35 m_{N^*}^{14} (s - m_{N^*}^2 + i m_{N^*} \Gamma_{N^*})}, \quad (39)$$

and with the same definitions used in Ref. [1],

$$\begin{aligned} \mathcal{M}_{9/2}^\pm = & \bar{u}_\Lambda \gamma_5 \{s \pm m_{N^*} (\not{p} + \not{k})\} \left[21 c_1 (3c_1^2 + c_2 c_3) \left\{ -p_{\Lambda\nu} + \frac{1}{s} c_\Lambda (p+k)_\nu \right\} - 3c_2 (7c_1^2 + c_2 c_3) \left\{ -k_\nu + \frac{1}{s} c_k (p+k)_\nu \right\} \right. \\ & + c_1 (7c_1^2 + 3c_2 c_3) \left\{ -\not{p}_\Lambda + \frac{1}{s} c_\Lambda (\not{p} + \not{k}) \right\} \left\{ -\gamma_\nu + \frac{1}{s} (\not{p} + \not{k})(p+k)_\nu \right\} - 3(7c_1^2 + c_2 c_3) \left\{ -\not{p}_\Lambda + \frac{1}{s} c_\Lambda (\not{p} + \not{k}) \right\} \\ & \times \left\{ -\not{k} + \frac{1}{s} c_k (\not{p} + \not{k}) \right\} \left\{ -p_{\Lambda\nu} + \frac{1}{s} c_\Lambda (p+k)_\nu \right\} + 6c_1 c_2 \left\{ -\not{p}_\Lambda + \frac{1}{s} c_\Lambda (\not{p} + \not{k}) \right\} \left\{ -\not{k} + \frac{1}{s} c_k (\not{p} + \not{k}) \right\} \\ & \times \left. \left\{ -k_\nu + \frac{1}{s} c_k (p+k)_\nu \right\} \right] [G^1 p^\nu (\not{k}\not{p} - \not{p}\not{k}) + G^2 (k^\nu p \cdot \epsilon - \epsilon^\nu p \cdot k) + G^3 (\epsilon^\nu \not{k} - k^\nu \not{p}) \not{p}] u_p, \quad (40) \end{aligned}$$

with a similar definition of G_1 , G_2 , and G_3 as in the case of spin-7/2 resonances, except in the case of spin-9/2 resonances the coupling constants G_1 , G_2 , and G_3 are multiplied by the regularization factor of $35s/63m_{N^*}^4$.

E. Decomposition of the scattering amplitude

As in our previous work [1], we decompose the scattering amplitude given by Eq. (36) into the gauge and Lorentz invariant matrices M_i ,

$$\mathcal{M} = \bar{u}_\Lambda \sum_{i=1}^6 A_i(s, t, u, k^2) M_i u_p, \quad (41)$$

where the gauge and Lorentz invariant matrices M_i are given by [13,14]

$$M_1 = \frac{1}{2} \gamma_5 (\not{p}\not{k} - \not{k}\not{p}), \quad (42)$$

$$M_2 = \gamma_5 [(2q - k) \cdot \epsilon P \cdot k - (2q - k) \cdot k P \cdot \epsilon], \quad (43)$$

$$M_3 = \gamma_5 (q_K \cdot k \not{p} - q \cdot \epsilon \not{k}), \quad (44)$$

$$M_4 = i \epsilon_{\mu\nu\rho\sigma} \gamma^\mu q^\nu \epsilon^\rho k^\sigma, \quad (45)$$

$$M_5 = \gamma_5 (q \cdot \epsilon k^2 - q \cdot k k \cdot \epsilon), \quad (46)$$

$$M_6 = \gamma_5 (k \cdot \epsilon \not{k} - k^2 \not{p}), \quad (47)$$

$$b_p = p \cdot k, \quad b_\Lambda = p_\Lambda \cdot k, \quad b_q = q \cdot k$$

$$c_p = (p+k) \cdot p, \quad c_\Lambda = (p+k) \cdot p_\Lambda, \quad c_k = (p+k) \cdot k,$$

$$c_s = 1 - \frac{1}{s} c_\Lambda, \quad c_1 = b_\Lambda - \frac{1}{s} c_\Lambda c_k, \quad c_2 = m_\Lambda^2 - \frac{1}{s} c_\Lambda^2,$$

$$c_3 = \frac{1}{s} c_k^2 - k^2, \quad c_4 = 2b_p + k^2, \quad c_5 = 4b_p + k^2.$$

The scattering amplitude for spin-9/2 nucleon resonances is obtained by using the same procedure as in the case of spin-7/2 resonances. The amplitude for spin-9/2 nucleon resonances can be written as

with $P = \frac{1}{2}(p + p_\Lambda)$, and $\epsilon_{\mu\nu\rho\sigma}$ is the four-dimensional Levi-Civita tensor with $\epsilon_{0123} = +1$. Note that for the sake of completeness, throughout this paper we give the formulation of electroproduction, where the values of k^2 and $k \cdot \epsilon$ are nonzero. For photoproduction, by setting k^2 and $k \cdot \epsilon$ to zero, obviously, only the matrices M_1 to M_4 exist.

The functions A_i depend on the Mandelstam variables and the square of virtual photon momentum. The functions are useful in the calculation of cross-section and polarization observables. The functions A_i for both spin-7/2 and -9/2 resonances are given in Appendix A.

Obviously, we can see that both spin-7/2 and spin-9/2 amplitudes have a similar pattern. This is different from the case of the spin-5/2 particle. On the other hand, the main difference between spin-7/2 and -9/2 amplitudes is that the momentum dependence increases as the spin number increases.

III. RESULTS AND DISCUSSION

The isobar model used in the present work is similar to that of previous work [1], except that in the present calculation it includes the four nucleon resonances with spins 7/2 and 9/2 listed in Table I. In total, we have used 21 nucleon resonances with spins ranging from 1/2 to 9/2 in our calculation.

As in the previous work [1] there are a number of unknown parameters both in the background and resonance terms. They are dominated by the coupling constants of

TABLE II. List of the background parameters, the hadronic form factor cutoffs, and the χ^2/N obtained in the present work compared with those obtained in our previous study [1]. Note that N is the number of fitted data points. Notation of the parameters is as in our previous studies [1,17].

Parameters	Present work	Previous work [1]
$g_{K\Lambda N}/\sqrt{4\pi}$	-3.00	-3.00
$g_{K\Sigma N}/\sqrt{4\pi}$	0.90	1.27
$G_{K^*}^V/4\pi$	-0.18	0.15
$G_{K^*}^T/4\pi$	0.72	0.26
$G_{K_1}^V/4\pi$	-0.63	1.46
$G_{K_1}^T/4\pi$	-2.94	0.07
$G_{\Lambda(1600)}/4\pi$	-7.19	8.41
$G_{\Lambda(1810)}/4\pi$	10.0	-9.61
Λ_B (GeV)	0.70	0.70
Λ_R (GeV)	1.18	1.31
θ_{had} (deg)	90.0	130
ϕ_{had} (deg)	0.01	177
χ^2/N	1.25	1.58

resonances and background terms. These parameters were varied by fitting the calculated observables to nearly 7400 experimental data points to produce the minimum χ^2/N value by using the CERN-MINUIT code [15].

The extracted background parameters are given in Table II, where we also display the corresponding parameters of our previous study for comparison. Since the leading coupling constants were varied within 20% of the SU(3) symmetry breaking, i.e., $g_{K\Lambda N}/\sqrt{4\pi} = -4.4$ to -3.0 and $g_{K\Sigma N}/\sqrt{4\pi} = 0.9$ to 1.3 , while the best fits were achieved by choosing the lowest values, it is obvious from Table II that the background terms are suppressed in both present and previous investigations. This conclusion is also supported by the fact that the extracted hadronic form factor cutoff of the Born terms is very soft, i.e., $\Lambda_B = 0.70$. Note that this cutoff value is the lowest allowed value during the fit process. The soft cutoffs found in the previous and present investigations might indicate the need for different types of form factor [16]. However, since our primary aim in this work is to investigate the effects of spin-7/2 and -9/2 nucleon resonances, we will address the problem of soft cutoffs in our future studies.

The resonance cutoff Λ_R is found to be larger than the background one. This indicates that the resonance contributions are not extremely suppressed. Nevertheless, Table II indicates that the suppression is greater in the present work, which is indicated by a smaller cutoff. This phenomenon can be understood, because the magnitude of the scattering amplitude increases after the inclusion of the spin-7/2 and -9/2 resonances. Therefore, to fit the observables the resonance cutoff must be decreased; i.e., the form factor suppression must be increased.

The coupling constants of hyperon resonances are large, both in previous and present works. This is consistent with

the finding of previous works, and we note that the two hyperon resonances are substantial to increase the values of the leading coupling constants [18].

Since the number of free parameters is larger in the present work, it is clear that the value of χ^2 of the present work is smaller. However, we note that the values of χ^2/N_{dof} in the previous and present works are 1.58 and 1.25, respectively, where $N_{\text{dof}} = N_{\text{data}} - N_{\text{par}}$, N_{data} is the number of fitted data, and N_{par} is the number of free parameters. This indicates that the inclusion of the four resonances with spins 7/2 and 9/2 still improves the performance of the present isobar model.

For completeness, we compare the fitted resonance coupling constants obtained in the present work with those of our previous work [1] in Table IV of Appendix B. Obviously, except for the difference between the two sets of coupling constants, there is no certain pattern in the coupling constants, which distinguishes the present work from the previous one. Nevertheless, we may conclude that the fit recalculates all couplings after the inclusion of spin-7/2 and 9/2 nucleon resonances. Furthermore, we also note that for higher spin resonances the corresponding coupling constants tend to be large, especially for the spin-9/2 ones. Presumably, this behavior originates from the regularization factor of s^4/m_N^8 in the propagator [see Eq. (28)], which severely suppresses the scattering amplitude due to the large resonance masses. A milder effect, but still significant, is found in the case of spin-5/2 resonances, where the regularization factor in the propagator is of s^2/m_N^4 [1,7,8].

A direct comparison between the presently obtained coupling constants with those available in the literature cannot be easily made because there exists a conceptual difference in their definitions [19,20]. It is obvious that in the present approach, known as the Breit-Wigner plus background parametrization approach in Ref. [20], the extracted coupling constants are model dependent; i.e., they depend on the number of resonances, hadronic form factors, energy-dependent widths, and other approximations used in the model. This is in contrast to the pole extraction method which is less model dependent [20]. We also note that in the most recent Review of Particle Properties of PDG [2,21], the properties of baryon resonances determined at the pole position are listed before those evaluated by using the Breit-Wigner approach. Furthermore, the extracted coupling constants given in Table IV of Appendix B are the product of electromagnetic and hadronic couplings. Different from the coupled-channels models, the present single-channel analysis cannot separate these couplings.

Nevertheless, as shown in Refs. [17,22], for a quick comparison we can calculate the relative decay widths $\sqrt{\Gamma_{\gamma N}\Gamma_{K^+\Lambda}}/\Gamma_{\text{total}}$ from the product of the electromagnetic and hadronic coupling constants and compare the result

TABLE III. The relative decay widths $\sqrt{\Gamma_{\gamma N} \Gamma_{K^+ \Lambda}} / \Gamma_{\text{total}}$ obtained in the present work compared to those listed by the PDG [2] and obtained in a constituent quark model (QM) [23]. The error bars listed in the last column (present work) are obtained from the MINUIT code.

Resonances	J^P	$\sqrt{\Gamma_{\gamma N} \Gamma_{K^+ \Lambda}} / \Gamma_{\text{total}} (\times 10^{-3})$		
		QM	PDG	Present work
$N(1650)$	$1/2^-$	$12.41^{+1.19}_{-3.34}$	9.17 ± 5.71	9.46 ± 0.04
$N(1675)$	$5/2^-$	0.00 ± 0.00	0.67 ± 0.67	11.09 ± 0.00
$N(1680)$	$5/2^+$	0.25 ± 0.00	...	0.20 ± 0.00
$N(1700)$	$3/2^-$	0.73 ± 0.36	2.12 ± 0.87	3.40 ± 0.01
$N(1710)$	$1/2^+$	1.15 ± 0.25	7.84 ± 6.30	3.93 ± 0.04
$N(1720)$	$3/2^+$	$4.26^{+0.69}_{-0.79}$	10.95 ± 8.41	10.13 ± 0.04
$N(1860)$	$5/2^+$	3.47 ± 0.03
$N(1875)$	$3/2^-$	3.27 ± 0.02
$N(1880)$	$1/2^+$	0.00 ± 0.00	...	7.84 ± 0.05
$N(1895)$	$1/2^-$	3.52 ± 0.10
$N(1900)$	$3/2^+$	87.49 ± 0.04
$N(2000)$	$5/2^+$	0.25 ± 0.15	...	2.95 ± 0.09
$N(2060)$	$5/2^-$	$0.71^{+0.10}_{-0.20}$...	65.47 ± 0.02
$N(2120)$	$3/2^-$	4.06 ± 0.02
$N(1990)$	$7/2^+$	0.00 ± 0.00	...	9.82 ± 0.01
$N(2190)$	$7/2^-$	$0.95^{+0.44}_{-0.29}$...	0.88 ± 0.02
$N(2220)$	$9/2^+$	0.18 ± 0.04	...	0.35 ± 0.00
$N(2250)$	$9/2^-$	0.00 ± 0.00	...	0.40 ± 0.07

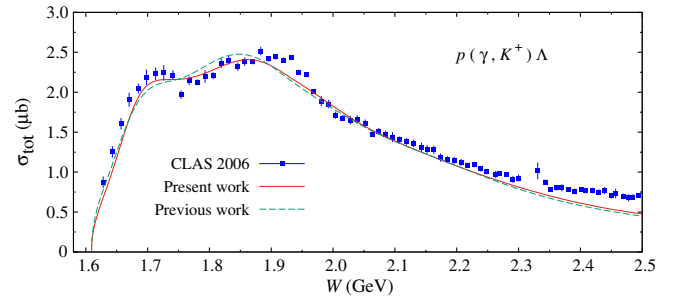


FIG. 2. Calculated total cross sections obtained in the previous [1] and present works compared with the experimental data from the CLAS Collaboration (solid squares [27]). Note that the experimental data shown in this figure are only for comparison and were not included in the fitting process.

with those obtained in a constituent quark model [23] and from the PDG [2].

The radiative or electromagnetic decay width to the γN channel can be obtained by using the formula given by PDG [2],

$$\Gamma_{\gamma N} = \frac{k^2}{\pi} \frac{2m_N}{(2J+1)m_{N^*}} (|A_{1/2}|^2 + |A_{3/2}|^2), \quad (48)$$

where k is the photon three-momentum in the resonance rest frame, J is the nucleon spin, and $A_{1/2}$ and $A_{3/2}$ are the electromagnetic decay amplitudes for their respective helicities or, in brief, the helicity amplitudes that can be calculated from the electromagnetic coupling constants as

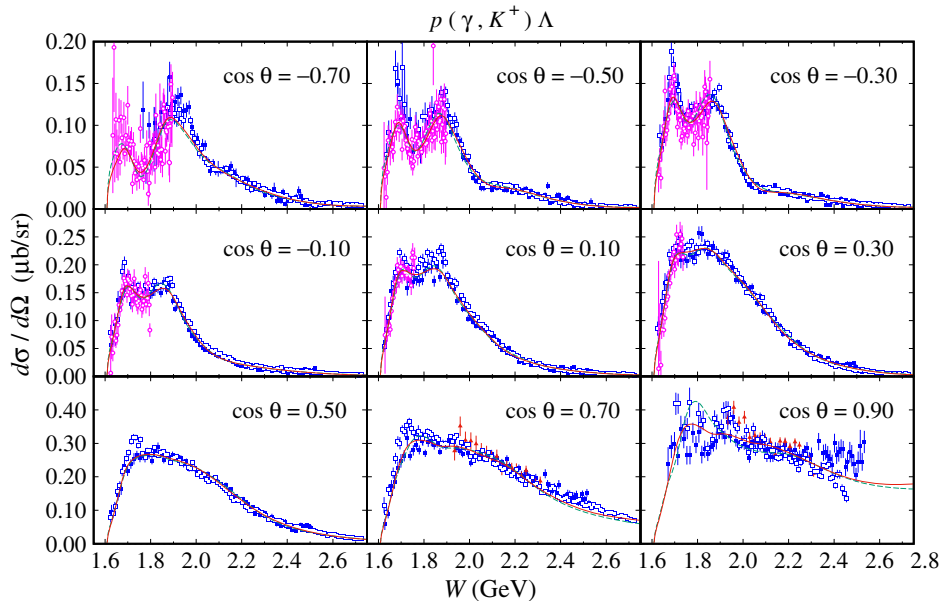


FIG. 3. Differential cross sections as a function of the total c.m. energy W for different values of the kaon c.m. angle. The corresponding value of $\cos \theta$ is given in each panel. Experimental data are from the CLAS Collaboration (solid squares [27] and open squares [28]), LEPS Collaboration (solid triangles [30]), and Crystal Ball Collaboration (open circles [31]). Notation of the curves is the same as in Fig. 2.

demonstrated in Appendix B. For the hadronic decay width to the $K^+\Lambda$ channel, we use [24]

$$\Gamma_{K^+\Lambda} = \frac{|\mathbf{q}|}{2\pi} \frac{2m_\Lambda}{(2J+1)m_{N^*}} |A_{K^+\Lambda}|^2, \quad (49)$$

where \mathbf{q} is the kaon momentum in the resonance rest frame and $A_{K^+\Lambda}$ is the hadronic decay amplitude that can be calculated by means of hadronic coupling constants.

In the case of spin-1/2 nucleon resonance we have simply [25]

$$A_{1/2} = -\frac{eg_1}{m_{N^*} + m_N} \sqrt{\frac{m_{N^*}^2 - m_N^2}{2m_N}}, \quad (50)$$

$$A_{K^+\Lambda} = -g_{K^+\Lambda N^*} \sqrt{\frac{E_\Lambda \mp m_\Lambda}{2m_\Lambda}}. \quad (51)$$

For nucleon resonances with spins 3/2 and higher, the formulas are given in Appendix B. As previously stated, since we cannot separate the extracted resonance coupling constants, we will use their product to calculate the relative decay width $\sqrt{\Gamma_{\gamma N} \Gamma_{K^+\Lambda}} / \Gamma_{\text{total}}$. The result is shown in Table III, where we also display the result obtained by the quark model [23] and from the PDG [2].

Table III indicates that, except for the $N(1675)$, the relative decay widths obtained in the present work are in good agreement with that of PDG. In fact, for both

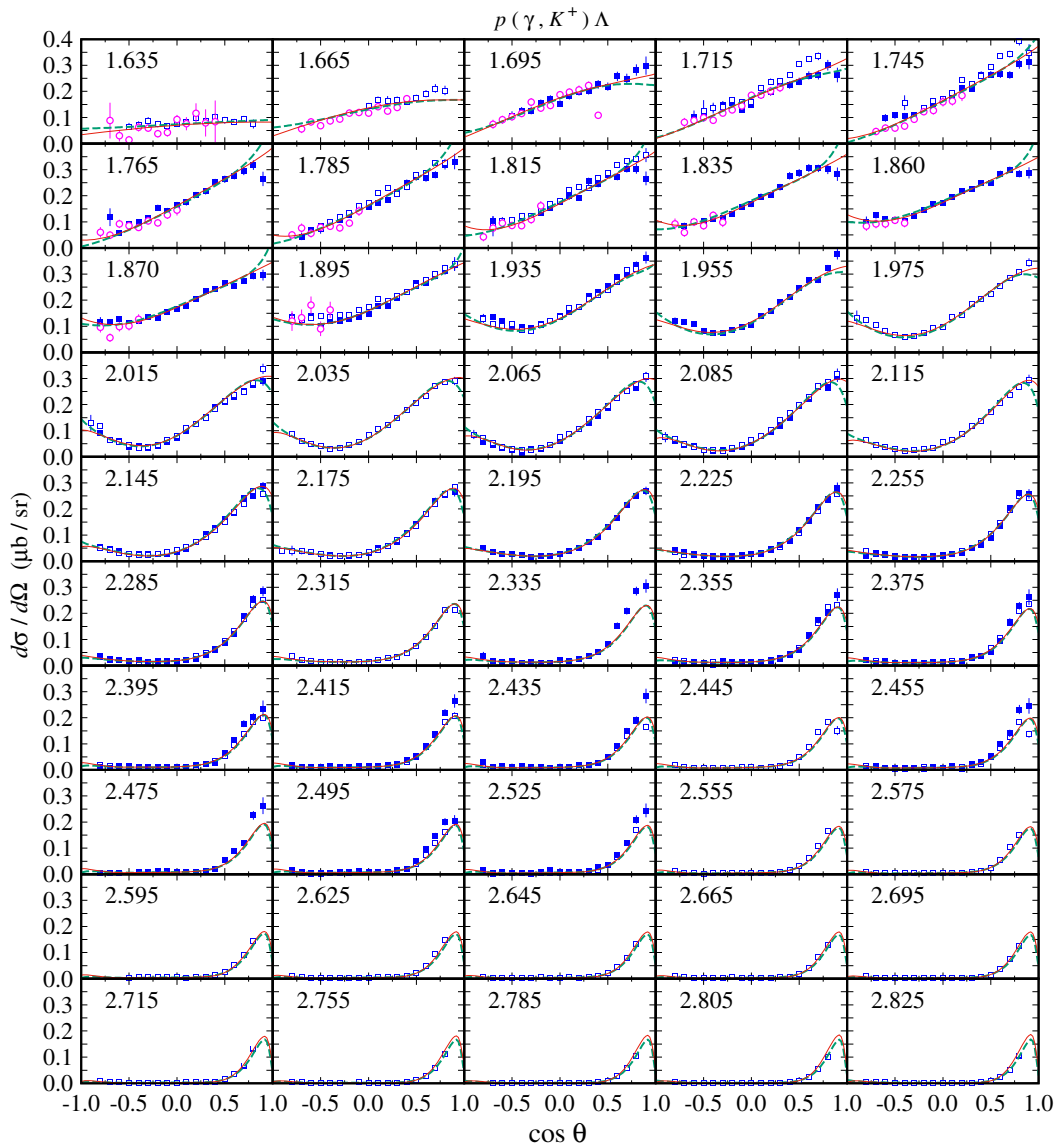


FIG. 4. The same as in Fig. 3, but for the angular distribution of the differential cross section with different values of the total c.m. energy W . The corresponding value of W in GeV is given in each panel.

$N(1650)$ and $N(1720)$ resonances the agreement is excellent. This result is important because we note that the two resonances are the well-established resonances with a four-star rating. In the case of $N(1700)$ and $N(1710)$ resonances we still obtain the same order of magnitude as the PDG values. By comparing our result to that of the quark model calculation [23], we can safely say that in most cases the relative decay widths are in the same order of magnitude.

Comparison between the extracted masses and widths of the resonances obtained in the present analysis and those of PDG is shown in Table V of Appendix D. Obviously, in almost all cases the extracted values are within the PDG limits. This is not too surprising, because during the fitting process we put the PDG values with their error bars as a constraint to the fitted parameters. In very rare cases, we have to slightly relax this limit in order to get the best χ^2 , e.g., in the case of $N(1440)$ total width. Note also that we add a 100 MeV error bar if it is not provided by PDG. This choice seems to be trivial, but we believe that this is quite fair since, as shown in Table V, the largest PDG error bar is 300 MeV.

Comparison between the calculated total cross sections from our present and previous works with experimental data is shown in Fig. 2. Although the total cross sections shown in Fig. 2 were not included during the fit process, sizable improvement is exhibited by the present model, especially at $W \approx 1.85$ GeV, where a missing $D_{13}(1895)$ was predicted almost two decades ago [17]. At this stage it is important to note that the peak around 1.85 GeV in the cross section was finally assigned as the $P_{13}(1900)$ state [26], instead of the $D_{13}(1895)$ one. Note also that the discrepancy between the calculated total cross sections and the CLAS 2006 data [27] is understandable, since the CLAS 2010 data [28] used in the fitting database tend to be smaller at this kinematics and also have smaller error bars. Obviously, the best fit would be achieved by reproducing the CLAS 2010 data [28]. In the latter, however, only a differential cross section and recoil polarization were reported.

More information can be explored from differential cross sections, as shown in Figs. 3 and 4. The energy distribution of the differential cross section displayed in Fig. 3 reveals the fact that the improvement is more apparent in the forward direction. Obviously, the experimental data are more scattered in this case. As a consequence, the best fit yields a democratic explanation of all available data, as clearly shown in Fig. 3, in the case of $\cos\theta = 0.90$. At this stage it is important to mention that the predicted cross sections of hypernuclear photoproduction and kaon photoproduction off a deuteron are very sensitive in this kinematics, since the dominant contribution comes from the forward region [29]. Therefore, a reliable description of the elementary cross section at this kinematics is urgently needed. Furthermore, an accurate cross-section

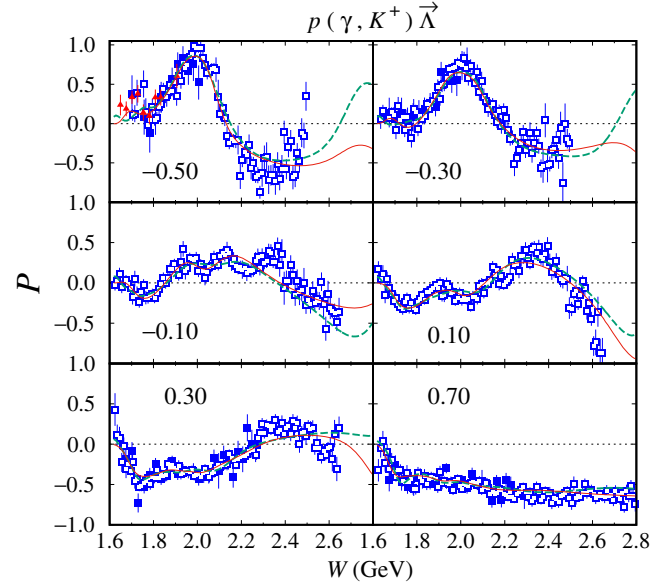


FIG. 5. Λ recoil polarization as a function of the total c.m. energy W for different values of the kaon c.m. angle. The corresponding value of $\cos\theta$ is given in each panel. Notation of the curves and experimental data is the same as in Fig. 3.

measurement at the forward directions would become the most challenging experiment in the future.

In the backward direction ($\cos\theta = -0.70$) we note that the inclusion of spin-7/2 and -9/2 nucleon resonances slightly improves the agreement between our model and experimental data. This is more apparent in Fig. 4, especially in the lower energy region, where the cross section tends to slightly increase as $\cos\theta$ approaches -1 .

Since the recoiled Λ decays into a nucleon and a pion, while the decay rate depends linearly on its polarization, the Λ polarization data can be obtained directly from experiments. In our previous works, these data were very important to reveal the existence of the narrow nucleon resonance at $W \approx 1650$ MeV [32]. The existence of this resonance was indicated by a sudden drop in the Λ polarization near 1650 MeV.

The energy and angular distributions of the recoiled Λ polarization are exhibited in Figs. 5 and 6, where we compare the results of the present and previous works with experimental data obtained by different collaborations. In Fig. 5 we can see that both results indicate the sudden drop of polarization, although no narrow resonance is included in both calculations. However, it is interesting to see that for $\cos\theta = 0.3$ both models cannot perfectly reproduce the experimental data. A thorough investigation of this subject will be considered in our future studies.

From Figs. 5 and 6 it is obvious that the improvement is more apparent at higher energies, which is understandable since the spin-7/2 and -9/2 nucleon resonances have

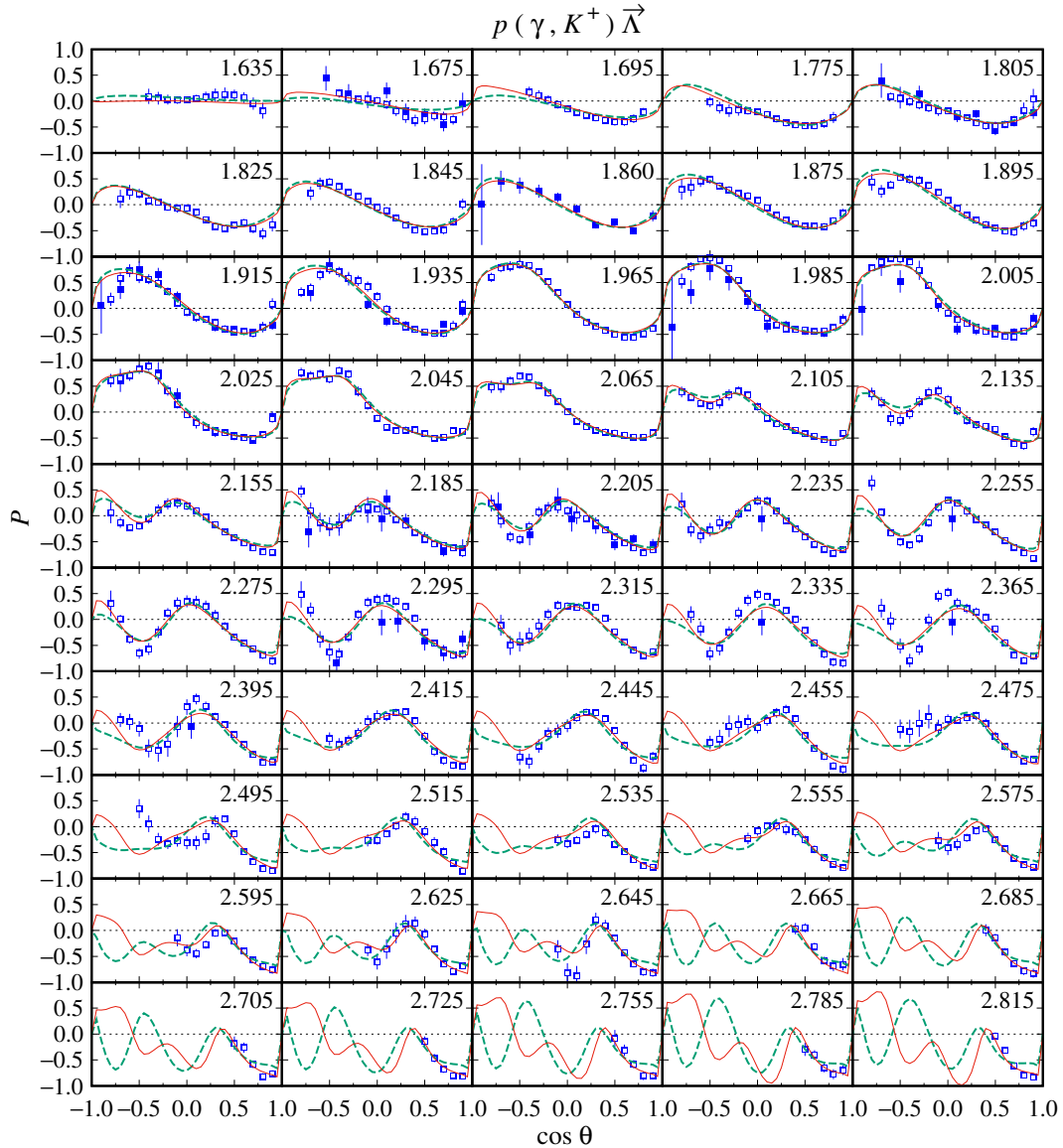


FIG. 6. The same as in Fig. 5, but for the angular distribution of Λ recoil polarization with different values of the total c.m. energy W . The corresponding value of W in GeV is given in each panel.

higher masses than the lower spin ones. Figure 6 shows that the predicted polarizations of the previous and present works are more distinguishable at high energies. At this kinematics the inclusion of spin-7/2 and -9/2 resonances slightly increases the number of oscillations, and the effect is more apparent at backward angles. Unfortunately, experimental data are only available near forward angles.

As mentioned in our previous work [1], the photon and target asymmetries could become a stringent constraint on the proliferation of phenomenological models that try to explain the kaon photoproduction data. This happens because the asymmetries depend sensitively on the ingredient of the scattering amplitude. Therefore, small changes in the fitted parameters could result in dramatic changes in these asymmetries.

We compare the calculated photon asymmetry of our present and previous works with experimental data in Figs. 7 and 8, whereas for the target asymmetry the comparison is given in Figs. 9 and 10. Clearly, the most significant improvement after the inclusion of the spin-7/2 and -9/2 resonances is obtained for these two asymmetries. In most cases shown in Figs. 7–10 the agreement of the calculated asymmetries and experimental data is substantially improved. Thus, we believe that the role played by the spin-7/2 and -9/2 resonances is more important in the case of photon and target asymmetries, rather than in the case of the differential cross section.

Finally, we show the comparison of phenomenological calculations and experimental data for the beam-recoil

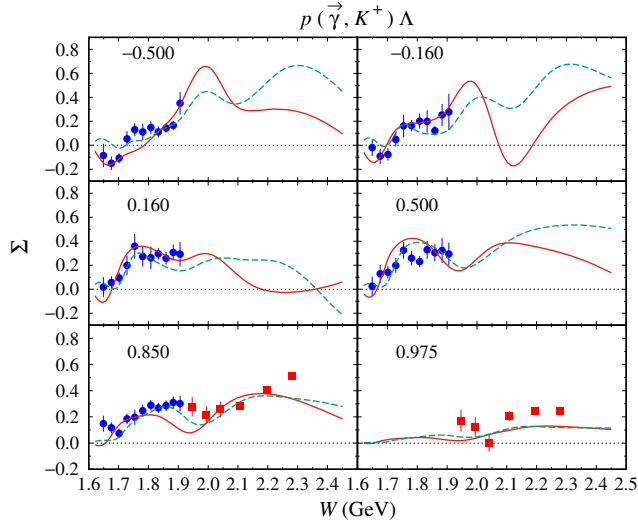


FIG. 7. Photon asymmetry as a function of the total c.m. energy W for different values of the kaon c.m. angle. The corresponding value of $\cos \theta$ is given in each panel. Notation of the curves is the same as in Fig. 2. Experimental data are from the LEPS Collaboration [30] (solid squares) and the GRAAL Collaboration [33] (solid circles).

double polarizations C_x , C_z , $O_{x'}$, and $O_{z'}$ in Figs. 11–18. In our previous work, we have stated that these observables are very interesting since experimental measurements indicate that the Λ hyperons are produced with 100% polarization as seen from the relation $R \equiv \sqrt{C_x^2 + C_y^2 + P^2} = 1.01 \pm 0.01$ [34]; i.e., all of the photon's helicities are transferred to the hyperon. To account for this phenomenon, a simple theoretical ansatz

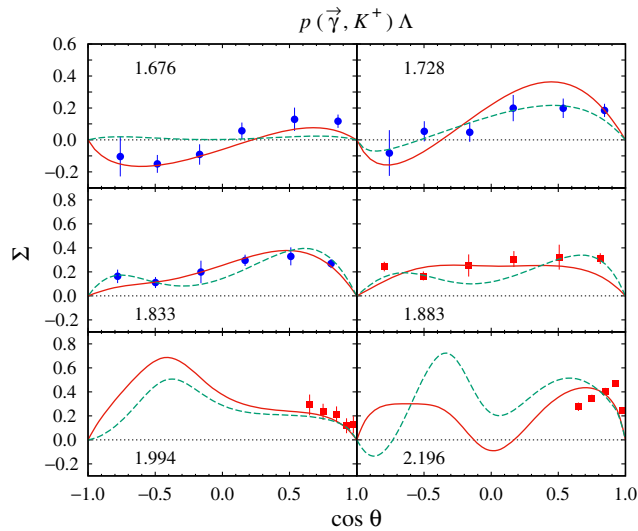


FIG. 8. The same as in Fig. 7, but for the angular distribution of photon asymmetry with different values of the total c.m. energy W . The corresponding value of W in GeV is given in each panel.

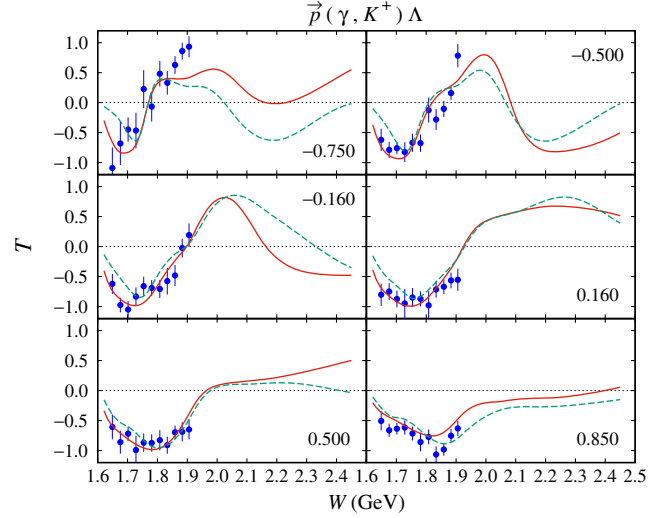


FIG. 9. Target asymmetry as a function of the total c.m. energy W for different values of the kaon c.m. angle. The corresponding value of $\cos \theta$ is given in each panel. Notation of the curves is as in Fig. 2. Experimental data are from the GRAAL Collaboration [33].

was proposed in Ref. [34]. In this framework, the photon undergoes a hadronization process and turns into a ϕ meson in a 3S_1 state. Thus, all of the photon “spin” can be successfully transferred to the created hyperon. However, in this ansatz the photoproduction process cannot excite a resonance (N^* or Δ) in the s -channel, and the predicted total polarization for the double polarizations $O_{x'}$ and $O_{z'}$, i.e., $R \equiv \sqrt{O_{x'}^2 + O_{y'}^2 + P^2} \approx 1$, is only partially fulfilled

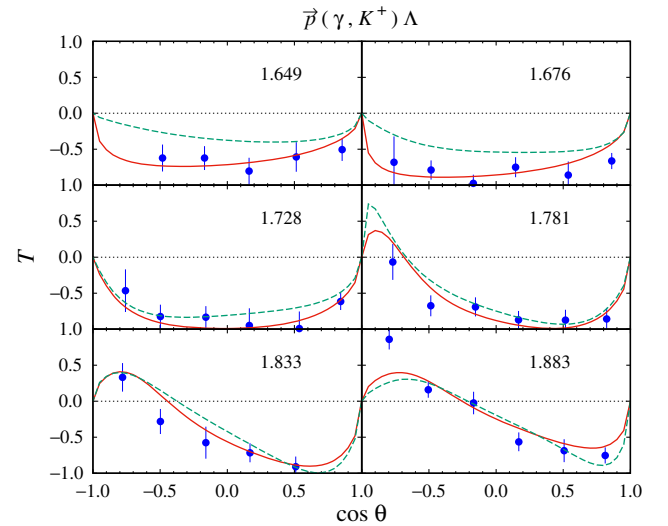


FIG. 10. The same as in Fig. 9, but for the angular distribution of the target asymmetry with different values of the total c.m. energy W . The corresponding value of W in GeV is given in each panel.

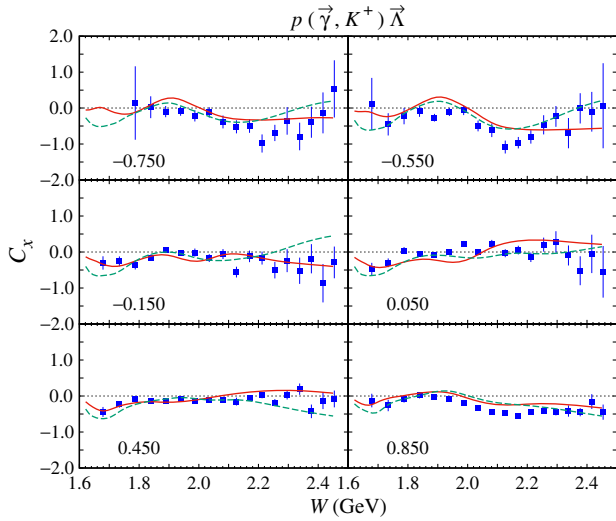


FIG. 11. Beam-recoil double polarization observable C_x as a function of the total c.m. energy W for different values of the kaon c.m. angle. The corresponding value of $\cos\theta$ is given in each panel. Notation of the curves is the same as in Fig. 2. Experimental data are from the CLAS Collaboration [36].

[35]. Therefore, further phenomenological or theoretical explanation to this end is urgently required. In view of the present work, where the nucleon resonances dominate the ingredient of scattering amplitude, we believe that it is important for the present isobar model to accurately reproduce the experimental data of these double-polarization observables.

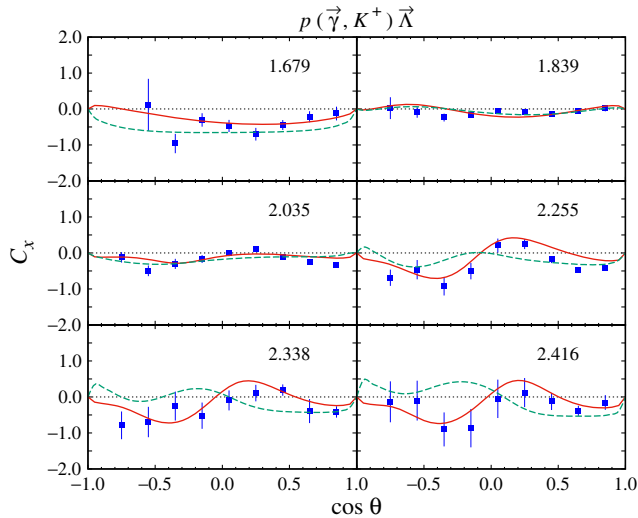


FIG. 12. The same as in Fig. 11, but for the angular distribution of the beam-recoil double polarization observable C_x with different values of the total c.m. energy W . The corresponding value of W in GeV is given in each panel.

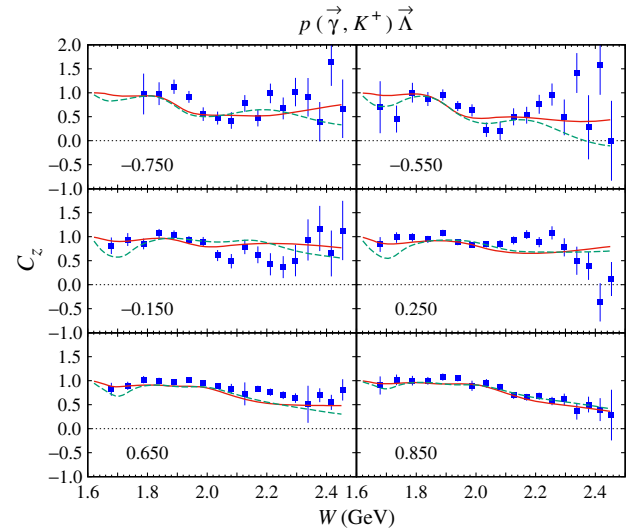


FIG. 13. The same as in Fig. 11, but for the beam-recoil double polarization observable C_z . The corresponding value of $\cos\theta$ is given in each panel.

In the previous work [1] we have nicely reproduced these observables. However, from Figs. 11–18, we can conclude that substantial improvement can still be achieved by including the spin-7/2 and -9/2 resonances in this isobar model. Especially in the case of double polarization C_x shown in Fig. 12, the angular distribution of this polarization can be perfectly reproduced within the experimental error bars. A similar result is obtained in the case of the O_x and O_z observables, as clearly shown in Figs. 16 and 18.

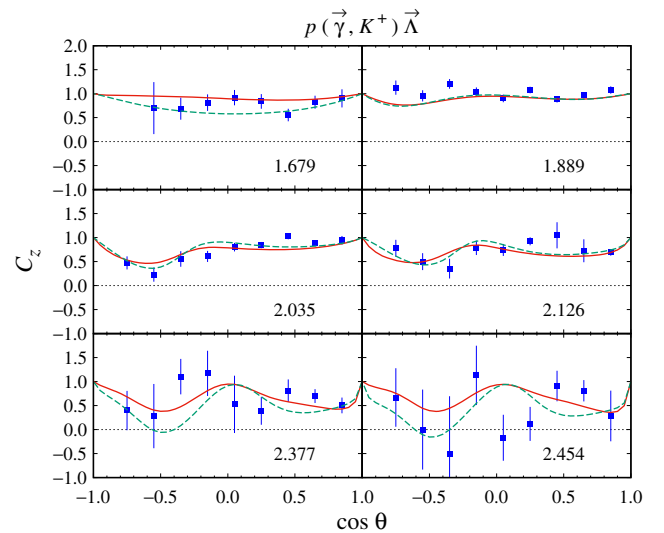


FIG. 14. The same as in Fig. 12, but for the beam-recoil double polarization observable C_z . The corresponding value of W in GeV is given in each panel.

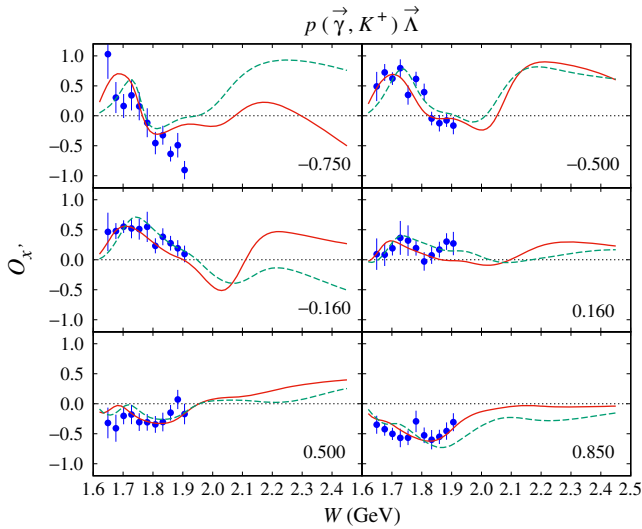


FIG. 15. Beam-recoil double polarization observable $O_{x'}$ as a function of the total c.m. energy W for different values of the kaon c.m. angle. The corresponding value of $\cos \theta$ is given in each panel. Notation of the curves is the same as in Fig. 2. Experimental data are from the GRAAL Collaboration [35].

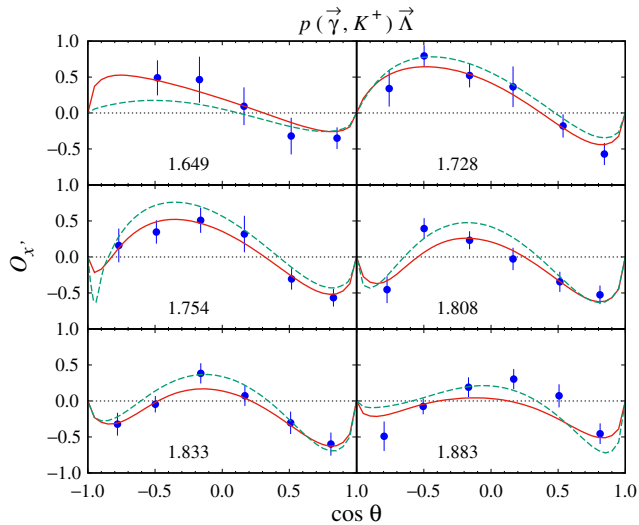


FIG. 16. The same as in Fig. 15, but for the angular distribution of the beam-recoil double polarization observable $O_{x'}$ with different values of the total c.m. energy W . The corresponding value of W in GeV is given in each panel.

IV. SUMMARY AND CONCLUSION

We have derived the formulas for spin-7/2 and -9/2 nucleon resonance amplitudes by using the gauge-invariant formulation proposed by Pascalutsa and Vrancx *et al.* These amplitudes were included in our previous isobar model of kaon photoproduction, and the model was refitted to the same experimental data used in the previous model. Two nucleon resonances with spin-7/2 and two nucleon resonances with spin-9/2 were taken into account in this study. Significant reduction of the χ^2/N value was obtained, and the agreement of the model calculation and experimental data was improved

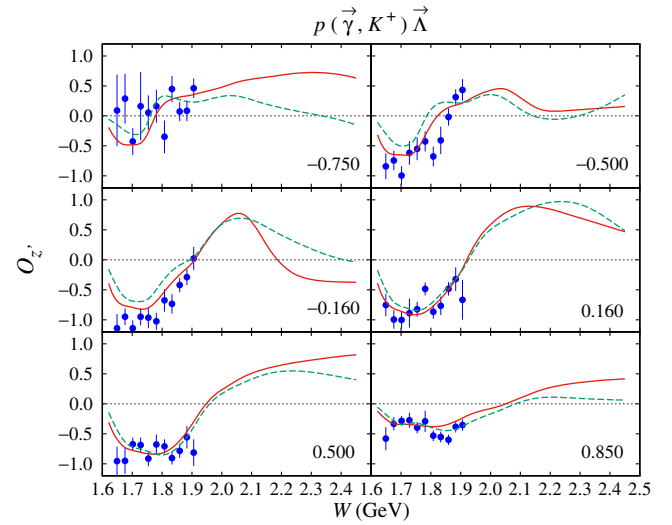


FIG. 17. The same as in Fig. 15, but for the beam-recoil double polarization observable $O_{z'}$. The corresponding value of $\cos \theta$ is given in each panel.

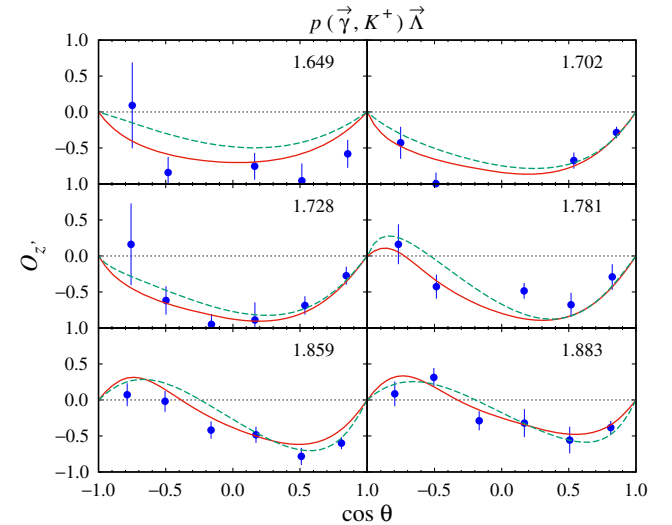


FIG. 18. The same as in Fig. 16, but for the beam-recoil double polarization observable $O_{z'}$. The corresponding value of W in GeV is given in each panel.

in almost all observables considered in the present study. A substantial improvement in the description of double polarization observables was observed after the inclusion of these resonances in our isobar model, i.e., the beam-recoil polarization C_x and C_z , as well as $O_{x'}$ and $O_{z'}$.

ACKNOWLEDGMENTS

This work was supported partly by the Research Cluster Grant of Universitas Indonesia, under Contract No. 1862/UN.R12/HKP.05.00/2015, and partly by the PITTA Grant of Universitas Indonesia, under Contract No. 689/UN2.R3.1/HKP.05.00/2017. S. C. would like to acknowledge the support from the Indonesian Endowment Fund for Education (LPDP).

APPENDIX A: FUNCTIONS A_i FOR SPIN-7/2 AND -9/2 RESONANCES

Note that in this appendix we use $m_N = m_p$. The extracted functions A_i given in Eq. (41) for spin-7/2 resonances can be written as

$$\begin{aligned}
A_1 = & \left[10c_1(7c_1^2 + 3c_2c_3)(s \pm m_{N^*}m_\Lambda) + 6(5c_1^2 + c_2c_3) \left\{ (m_\Lambda^2 c_k - b_p c_\Lambda) \pm m_{N^*} m_\Lambda \left(\frac{1}{s} c_k c_\Lambda - b_p \right) \right\} \right] G_1 \\
& + \frac{1}{2}(m_p + m_\Lambda) \left[\left\{ (m_p c_\Lambda - m_\Lambda c_p) \pm m_{N^*} \left(m_p m_\Lambda - \frac{1}{s} c_\Lambda c_p \right) \right\} \left\{ 10c_1(c_1 - b_p c_s) - \frac{2}{s} k^2 c_2 c_p + (5c_1^2 + c_2c_3) \right\} \right. \\
& - b_p \left(m_\Lambda \pm \frac{1}{s} m_{N^*} c_\Lambda \right) (5c_1^2 + c_2c_3) \pm 5m_{N^*} \left\{ (c_1 - b_p c_s)(7c_1^2 + c_2c_3) - \frac{2}{s} k^2 c_1 c_2 c_p \right\} \left. \right] G_2 + m_p \left[\frac{1}{2}(m_p + m_\Lambda) \right. \\
& \times \left\{ (s \pm m_{N^*} m_p) \left[-5c_s(7c_1^2 + c_2c_3) - 10c_1 c_2 \frac{1}{s} c_k \right] - \left[(m_p m_\Lambda + 7c_\Lambda) \pm m_{N^*} \left(\frac{1}{s} m_p c_\Lambda + 7m_\Lambda \right) \right] (5c_1^2 + c_2c_3) \right. \\
& - \left. \left[(b_p c_\Lambda - m_p m_\Lambda c_k) \pm m_{N^*} \left(m_\Lambda b_p - \frac{1}{s} m_p c_\Lambda c_k \right) \right] \left(-10c_1 c_s - 2c_2 \frac{1}{s} c_k \right) \right\} + \left\{ (4m_p c_\Lambda + 4m_\Lambda c_p + m_\Lambda c_k) \right. \\
& \left. \pm m_{N^*} \left(4m_p m_\Lambda + \frac{4}{s} c_p c_\Lambda + \frac{1}{s} c_k c_\Lambda \right) \right\} (5c_1^2 + c_2c_3) \mp 5m_{N^*} c_1 (7c_1^2 + 3c_2c_3) \left. \right] G_3, \tag{A1}
\end{aligned}$$

$$\begin{aligned}
A_2 = & \frac{1}{t - m_K^2} \left\{ -12k^2(5c_1^2 + c_2c_3)(c_\Lambda \pm m_{N^*} m_\Lambda) G_1 + \left[5(s \mp m_{N^*} m_p) \left\{ (c_1 - b_p c_s)(7c_1^2 + c_2c_3) - \frac{2}{s} k^2 c_1 c_2 c_p \right\} \right. \right. \\
& - m_p k^2 \left(m_\Lambda \pm \frac{1}{s} m_{N^*} c_\Lambda \right) (5c_1^2 + c_2c_3) + 2 \left\{ (m_p m_\Lambda c_k - b_p c_\Lambda) \pm m_{N^*} \left(\frac{1}{s} m_p c_\Lambda c_k - m_\Lambda b_p \right) \right\} \\
& \times \left. \left\{ 5c_1(b_p c_s - c_1) + \frac{1}{s} k^2 c_2 c_p \right\} \right] G_2 \\
& + m_p \left[\left(m_\Lambda \pm \frac{1}{s} m_{N^*} c_\Lambda \right) \left\{ k^2 \left(5c_1^2 + c_2c_3 - \frac{4}{s} c_2 c_k c_p \right) + 20c_1 c_k (c_1 - b_p c_s) \right\} \right. \\
& + 2k^2 \left\{ (m_p c_\Lambda + m_\Lambda c_p) \pm m_{N^*} \left(m_p m_\Lambda + \frac{1}{s} c_\Lambda c_p \right) \right\} \left(5c_1 c_s + \frac{1}{s} c_2 c_k \right) \\
& \left. \pm 5m_{N^*} \left\{ (7c_1^2 + c_2c_3)(k^2 c_s - 2b_q) - c_1 c_2 k^2 \left(2 + \frac{2}{s} c_p \right) \right\} \right] G_3 \left. \right\}, \tag{A2}
\end{aligned}$$

$$\begin{aligned}
A_3 = & \left[6c_k(5c_1^2 + c_2c_3) \left(m_\Lambda \pm \frac{1}{s} m_{N^*} c_\Lambda \right) \pm 10m_{N^*} c_1 (7c_1^2 + 3c_2c_3) \right] G_1 \\
& + \frac{1}{2} \left[\left\{ (m_p c_\Lambda - m_\Lambda c_p) \pm m_{N^*} \left(m_p m_\Lambda - \frac{1}{s} c_\Lambda c_p \right) \right\} \left\{ 10c_1 \left(c_1 + b_p \left(1 + \frac{1}{s} c_\Lambda \right) \right) - \frac{2}{s} k^2 c_2 c_p + (5c_1^2 + c_2c_3) \right\} \right. \\
& - b_p \left(m_\Lambda \pm \frac{1}{s} m_{N^*} c_\Lambda \right) (5c_1^2 + c_2c_3) \pm 5m_{N^*} \left\{ \left(c_1 + b_p \left(1 + \frac{1}{s} c_\Lambda \right) \right) (7c_1^2 + c_2c_3) - \frac{2}{s} k^2 c_1 c_2 c_p \right\} \left. \right] G_2 \\
& + \frac{1}{2} m_p \left[5(s \pm m_{N^*} m_p) \left\{ \left(1 + \frac{1}{s} c_\Lambda \right) (7c_1^2 + c_2c_3) - 2c_1 c_2 \frac{1}{s} c_k \right\} \right. \\
& - \left\{ (m_p m_\Lambda + 7c_\Lambda) \pm m_{N^*} \left(\frac{1}{s} m_p c_\Lambda + 7m_\Lambda \right) \right\} (5c_1^2 + c_2c_3) - \left\{ (b_p c_\Lambda - m_p m_\Lambda c_k) \pm m_{N^*} \left(m_\Lambda b_p - \frac{1}{s} m_p c_\Lambda c_k \right) \right\} \\
& \times \left. \left\{ 10c_1 \left(1 + \frac{1}{s} c_\Lambda \right) - 2c_2 \frac{1}{s} c_k \right\} \right] G_3, \tag{A3}
\end{aligned}$$

$$\begin{aligned}
A_4 = & \left[6c_k(5c_1^2 + c_2c_3) \left(m_\Lambda \pm \frac{1}{s} m_{N^*} c_\Lambda \right) \pm 10m_{N^*} c_1(7c_1^2 + 3c_2c_3) \right] G_1 \\
& + \frac{1}{2} \left[\left\{ (m_p c_\Lambda - m_\Lambda c_p) \pm m_{N^*} \left(m_p m_\Lambda - \frac{1}{s} c_\Lambda c_p \right) \right\} \left\{ 10c_1(c_1 - b_p c_s) - \frac{2}{s} k^2 c_2 c_p + (5c_1^2 + c_2c_3) \right\} \right. \\
& - b_p \left(m_\Lambda \pm \frac{1}{s} m_{N^*} c_\Lambda \right) (5c_1^2 + c_2c_3) \pm 5m_{N^*} \left\{ (c_1 - b_p c_s)(7c_1^2 + c_2c_3) - \frac{2}{s} k^2 c_1 c_2 c_p \right\} \left. \right] G_2 \\
& + \frac{1}{2} m_p \left[5(s \pm m_{N^*} m_p) \left\{ -c_s(7c_1^2 + c_2c_3) - 2c_1 c_2 \frac{1}{s} c_k \right\} - \left\{ (m_p m_\Lambda + 7c_\Lambda) \pm m_{N^*} \left(\frac{1}{s} m_p c_\Lambda + 7m_\Lambda \right) \right\} (5c_1^2 + c_2c_3) \right. \\
& - \left. \left\{ (b_p c_\Lambda - m_p m_\Lambda c_k) \pm m_{N^*} \left(m_\Lambda b_p - \frac{1}{s} m_p c_\Lambda c_k \right) \right\} \times \left(-10c_1 c_s - 2c_2 \frac{1}{s} c_k \right) \right] G_3, \tag{A4}
\end{aligned}$$

$$\begin{aligned}
A_5 = & \frac{1}{t - m_K^2} \left\{ 6c_5(5c_1^2 + c_2c_3)(c_\Lambda \pm m_{N^*} m_\Lambda) G_1 \right. \\
& + \frac{1}{2} \left[5(s \mp m_{N^*} m_p) \left\{ - \left(b_p + b_\Lambda - \frac{1}{s} c_\Lambda c_5 \right) (7c_1^2 + c_2c_3) + \frac{2}{s} c_1 c_2 c_5 c_p \right\} + m_p c_5 \left(m_\Lambda \pm \frac{1}{s} m_{N^*} c_\Lambda \right) (5c_1^2 + c_2c_3) \right. \\
& + 2 \left\{ (m_p m_\Lambda c_k - b_p c_\Lambda) \pm m_{N^*} \left(\frac{1}{s} m_p c_\Lambda c_k - m_\Lambda b_p \right) \right\} \times \left\{ 5c_1 \left(b_p + b_\Lambda - \frac{1}{s} c_\Lambda c_5 \right) - \frac{1}{s} c_2 c_p c_5 \right\} \left. \right] G_2 \\
& + m_p \left[-\frac{1}{2} \left(m_\Lambda \pm \frac{1}{s} m_{N^*} c_\Lambda \right) \left\{ c_5 \left(5c_1^2 + c_2c_3 - \frac{4}{s} c_2 c_k c_p \right) + 20c_1 c_k \left(b_p + b_\Lambda - \frac{1}{s} c_\Lambda c_5 \right) \right\} \right. \\
& - \left. \left\{ (m_p c_\Lambda + m_\Lambda c_p) \pm m_{N^*} \left(m_p m_\Lambda + \frac{1}{s} c_\Lambda c_p \right) \right\} \left(5c_1 \left(4b_\Lambda - k^2 - \frac{1}{s} c_\Lambda c_5 \right) + \frac{1}{s} c_2 c_5 c_k \right) \right. \\
& \left. \pm 5m_{N^*} \left\{ \frac{1}{2} (7c_1^2 + c_2c_3) \left(k^2 - 2b_q + \frac{1}{s} c_\Lambda c_5 \right) + c_1 c_2 c_5 \left(1 + \frac{1}{s} c_p \right) \right\} \right] G_3 \left. \right\}, \tag{A5}
\end{aligned}$$

$$\begin{aligned}
A_6 = & \left[6\{ (m_\Lambda s + m_p c_\Lambda) \pm m_{N^*} (c_\Lambda + m_p m_\Lambda) \} (5c_1^2 + c_2c_3) \right] G_1 \\
& + \frac{1}{2} \left[\left\{ (m_p c_\Lambda - m_\Lambda c_p) \pm m_{N^*} \left(m_p m_\Lambda - \frac{1}{s} c_\Lambda c_p \right) \right\} \left\{ (5c_1^2 + c_2c_3) + 10c_1(c_1 + b_p c_s) - \frac{2}{s} c_2 c_4 c_p \right\} \right. \\
& + b_p \left(m_\Lambda \pm \frac{1}{s} m_{N^*} c_\Lambda \right) (5c_1^2 + c_2c_3) \pm 5m_{N^*} \left\{ (7c_1^2 + c_2c_3)(c_1 + b_p c_s) - \frac{2}{s} c_1 c_2 c_4 c_p \right\} \left. \right] G_2 \\
& + \frac{1}{2} m_p \left[5(s \pm m_{N^*} m_p) \left\{ (7c_1^2 + c_2c_3) c_s - 2c_1 c_2 \left(1 + \frac{1}{s} c_p \right) \right\} + (5c_1^2 + c_2c_3) \right. \\
& \times \left. \left\{ (m_p m_\Lambda - 5c_\Lambda) \pm m_{N^*} \left(\frac{1}{s} m_p c_\Lambda - 5m_\Lambda \right) \right\} \right. \\
& + 2 \left\{ 5c_1 c_s + c_2 \left(1 + \frac{1}{s} c_p \right) \right\} \left\{ (m_p m_\Lambda c_k - b_p c_\Lambda) \pm m_{N^*} \left(\frac{1}{s} m_p c_\Lambda c_k - m_\Lambda b_p \right) \right\} \left. \right] G_3. \tag{A6}
\end{aligned}$$

For spin-9/2 resonances the functions are given by

$$\begin{aligned}
 A_1 = & \left[6(21c_1^4 + 14c_1^2c_2c_3 + c_2^2c_3^2)(-s \pm m_{N^*}m_\Lambda) + 8c_1(7c_1^2 + 3c_2c_3) \left\{ -(m_\Lambda^2c_k - b_p c_\Lambda) \pm m_{N^*}m_\Lambda \left(\frac{1}{s}c_k c_\Lambda - b_p \right) \right\} \right] G_1 \\
 & + \frac{1}{2}(m_p + m_\Lambda) \left[\left\{ -(m_p c_\Lambda - m_\Lambda c_p) \pm m_{N^*} \left(m_p m_\Lambda - \frac{1}{s}c_\Lambda c_p \right) \right\} \right. \\
 & \times \left\{ 3(7c_1^2 + c_2c_3)(c_1 - b_p c_s) - \frac{6}{s}k^2c_1c_2c_p + c_1(7c_1^2 + 3c_2c_3) \right\} - b_p \left(-m_\Lambda \pm \frac{1}{s}m_{N^*}c_\Lambda \right) c_1(7c_1^2 + 3c_2c_3) \\
 & \left. \pm m_{N^*} \left\{ 21c_1(c_1 - b_p c_s)(3c_1^2 + c_2c_3) - \frac{3}{s}k^2c_2c_p(7c_1^2 + c_2c_3) \right\} \right] G_2 \\
 & + m_p \left[\frac{1}{2}(m_p + m_\Lambda) \left\{ (-s \pm m_{N^*}m_p) \left[-21c_s c_1(3c_1^2 + c_2c_3) - 3\frac{1}{s}c_2c_k(7c_1^2 + c_2c_3) \right] \right. \right. \\
 & \left. \left. - c_1 \left[-(m_p m_\Lambda + 9c_\Lambda) \pm m_{N^*} \left(\frac{1}{s}m_p c_\Lambda + 9m_\Lambda \right) \right] (7c_1^2 + 3c_2c_3) \right. \right. \\
 & \left. \left. + 3 \left[-(b_p c_\Lambda - m_p m_\Lambda c_k) \pm m_{N^*} \left(m_\Lambda b_p - \frac{1}{s}m_p c_\Lambda c_k \right) \right] \left[c_s(7c_1^2 + c_2c_3) + \frac{2}{s}c_1c_2c_k \right] \right\} \right. \\
 & \left. + c_1 \left\{ -(5m_p c_\Lambda + 5m_\Lambda c_p + m_\Lambda c_k) \pm m_{N^*} \left(5m_p m_\Lambda + \frac{5}{s}c_p c_\Lambda + \frac{1}{s}c_k c_\Lambda \right) \right\} (7c_1^2 + 3c_2c_3) \right. \\
 & \left. \mp 3m_{N^*}(21c_1^4 + 14c_1^2c_2c_3 + c_2^2c_3^2) \right] G_3, \tag{A7}
 \end{aligned}$$

$$\begin{aligned}
 A_2 = & \frac{1}{t - m_K^2} \left\{ -16k^2c_1(7c_1^2 + 3c_2c_3)(-c_\Lambda \pm m_{N^*}m_\Lambda)G_1 \right. \\
 & + \left[3(s \pm m_{N^*}m_p) \left\{ 7c_1(b_p c_s - c_1)(3c_1^2 + c_2c_3) + \frac{1}{s}k^2c_2c_p(7c_1^2 + c_2c_3) \right\} - m_p k^2c_1 \left(-m_\Lambda \pm \frac{1}{s}m_{N^*}c_\Lambda \right) (7c_1^2 + 3c_2c_3) \right. \\
 & \left. + 3 \left\{ -(m_p m_\Lambda c_k - b_p c_\Lambda) \pm m_{N^*} \left(\frac{1}{s}m_p c_\Lambda c_k - m_\Lambda b_p \right) \right\} \times \left\{ (7c_1^2 + c_2c_3)(b_p c_s - c_1) + \frac{2}{s}k^2c_1c_2c_p \right\} \right] G_2 \\
 & + m_p \left[\left(-m_\Lambda \pm \frac{1}{s}m_{N^*}c_\Lambda \right) \left\{ k^2c_1(7c_1^2 + 3c_2c_3) + 6c_k(c_1 - b_p c_s) \times (7c_1^2 + c_2c_3) - \frac{12}{s}k^2c_1c_2c_k c_p \right\} \right. \\
 & \left. + 3k^2 \left\{ -(m_p c_\Lambda + m_\Lambda c_p) \pm m_{N^*} \left(m_p m_\Lambda + \frac{1}{s}c_\Lambda c_p \right) \right\} \left\{ c_s(7c_1^2 + c_2c_3) + \frac{2}{s}c_1c_2c_k \right\} \right. \\
 & \left. \pm m_{N^*} \left\{ 21c_1(3c_1^2 + c_2c_3)(k^2c_s - 2b_q) - 3k^2c_2 \left(1 + \frac{1}{s}c_p \right) (7c_1^2 + c_2c_3) \right\} \right] G_3 \left. \right\}, \tag{A8}
 \end{aligned}$$

$$\begin{aligned}
 A_3 = & \left[8c_k c_1(7c_1^2 + 3c_2c_3) \left(-m_\Lambda \pm \frac{1}{s}m_{N^*}c_\Lambda \right) \pm 6m_{N^*}(21c_1^4 + 14c_1^2c_2c_3 + c_2^2c_3^2) \right] G_1 \\
 & + \frac{1}{2} \left[\left\{ -(m_p c_\Lambda - m_\Lambda c_p) \pm m_{N^*} \left(m_p m_\Lambda - \frac{1}{s}c_\Lambda c_p \right) \right\} \left\{ 3(7c_1^2 + c_2c_3) \left(c_1 + b_p \left(1 + \frac{1}{s}c_\Lambda \right) \right) - \frac{6}{s}k^2c_1c_2c_p + c_1(7c_1^2 + 3c_2c_3) \right\} \right. \\
 & \left. + b_p c_1 \left(m_\Lambda \mp \frac{1}{s}m_{N^*}c_\Lambda \right) (7c_1^2 + 3c_2c_3) \pm 3m_{N^*} \left\{ 7c_1 \left(c_1 + b_p \left(1 + \frac{1}{s}c_\Lambda \right) \right) (3c_1^2 + c_2c_3) - \frac{1}{s}k^2c_2c_p(7c_1^2 + c_2c_3) \right\} \right] G_2 \\
 & + \frac{1}{2}m_p \left[3(s \mp m_{N^*}m_p) \left\{ \frac{1}{s}c_2c_k(7c_1^2 + c_2c_3) - 7c_1 \left(1 + \frac{1}{s}c_\Lambda \right) (3c_1^2 + c_2c_3) \right\} \right. \\
 & \left. + c_1 \left\{ (m_p m_\Lambda + 9c_\Lambda) \mp m_{N^*} \left(\frac{1}{s}m_p c_\Lambda + 9m_\Lambda \right) \right\} (7c_1^2 + 3c_2c_3) + 3 \left\{ (b_p c_\Lambda - m_p m_\Lambda c_k) \pm m_{N^*} \left(\frac{1}{s}m_p c_\Lambda c_k - m_\Lambda b_p \right) \right\} \right. \\
 & \left. \times \left\{ \left(1 + \frac{1}{s}c_\Lambda \right) (7c_1^2 + c_2c_3) - \frac{2}{s}c_1c_2c_k \right\} \right] G_3, \tag{A9}
 \end{aligned}$$

$$\begin{aligned}
A_4 = & \left[8c_k c_1 (7c_1^2 + 3c_2 c_3) \left(-m_\Lambda \pm \frac{1}{s} m_{N^*} c_\Lambda \right) \pm 6m_{N^*} (21c_1^4 + 14c_1^2 c_2 c_3 + c_2^2 c_3^2) \right] G_1 \\
& + \frac{1}{2} \left[\left\{ -(m_p c_\Lambda - m_\Lambda c_p) \pm m_{N^*} \left(m_p m_\Lambda - \frac{1}{s} c_\Lambda c_p \right) \right\} \left\{ 3(7c_1^2 + c_2 c_3) (c_1 - b_p c_s) - \frac{6}{s} k^2 c_1 c_2 c_p + c_1 (7c_1^2 + 3c_2 c_3) \right\} \right. \\
& - b_p c_1 \left(-m_\Lambda \pm \frac{1}{s} m_{N^*} c_\Lambda \right) (7c_1^2 + 3c_2 c_3) \pm 3m_{N^*} \left\{ 7c_1 (c_1 - b_p c_s) (3c_1^2 + c_2 c_3) - \frac{1}{s} k^2 c_2 c_p (7c_1^2 + c_2 c_3) \right\} \left. \right] G_2 \\
& + \frac{1}{2} m_p \left[3(-s \pm m_{N^*} m_p) \left\{ -7c_1 c_s (3c_1^2 + c_2 c_3) - \frac{1}{s} c_2 c_k (7c_1^2 + c_2 c_3) \right\} \right. \\
& - c_1 \left\{ -(m_p m_\Lambda + 9c_\Lambda) \pm m_{N^*} \left(\frac{1}{s} m_p c_\Lambda + 9m_\Lambda \right) \right\} (7c_1^2 + 3c_2 c_3) \\
& \left. + 3 \left\{ (b_p c_\Lambda - m_p m_\Lambda c_k) \pm m_{N^*} \left(\frac{1}{s} m_p c_\Lambda c_k - m_\Lambda b_p \right) \right\} \left\{ -c_s (7c_1^2 + c_2 c_3) - \frac{2}{s} c_1 c_2 c_k \right\} \right] G_3, \tag{A10}
\end{aligned}$$

$$\begin{aligned}
A_5 = & \frac{1}{t - m_K^2} \left\{ 8c_1 c_5 (7c_1^2 + 3c_2 c_3) (-c_\Lambda \pm m_{N^*} m_\Lambda) G_1 \right. \\
& + \frac{1}{2} \left[3(s \pm m_{N^*} m_p) \left\{ 7c_1 \left(b_p + b_\Lambda - \frac{1}{s} c_\Lambda c_5 \right) (3c_1^2 + c_2 c_3) - \frac{1}{s} c_2 c_5 c_p (7c_1^2 + c_2 c_3) \right\} \right. \\
& + m_p c_1 c_5 \left(-m_\Lambda \pm \frac{1}{s} m_{N^*} c_\Lambda \right) (7c_1^2 + 3c_2 c_3) \\
& + 3 \left\{ -(m_p m_\Lambda c_k - b_p c_\Lambda) \pm m_{N^*} \left(\frac{1}{s} m_p c_\Lambda c_k - m_\Lambda b_p \right) \right\} \left\{ (7c_1^2 + c_2 c_3) \left(b_p + b_\Lambda - \frac{1}{s} c_\Lambda c_5 \right) - \frac{2}{s} c_1 c_2 c_5 c_p \right\} \left. \right] G_2 \\
& + m_p \left[\left(m_\Lambda \mp \frac{1}{s} m_{N^*} c_\Lambda \right) \left\{ \frac{1}{2} c_1 c_5 (7c_1^2 + 3c_2 c_3) + 3c_k \left(b_p + b_\Lambda - \frac{1}{s} c_\Lambda c_5 \right) (7c_1^2 + c_2 c_3) - \frac{6}{s} c_1 c_2 c_5 c_k c_p \right\} \right. \\
& + \frac{3}{2} \left\{ (m_p c_\Lambda + m_\Lambda c_p) \mp m_{N^*} \left(m_p m_\Lambda + \frac{1}{s} c_\Lambda c_p \right) \right\} \left\{ \left(4b_\Lambda - k^2 - \frac{1}{s} c_\Lambda c_5 \right) (7c_1^2 + c_2 c_3) + \frac{2}{s} c_1 c_2 c_5 c_k \right\} \\
& \left. \pm \frac{3}{2} m_{N^*} \left\{ 7c_1 (3c_1^2 + c_2 c_3) \left(k^2 - 2b_q + \frac{1}{s} c_\Lambda c_5 \right) + c_2 c_5 \left(1 + \frac{1}{s} c_p \right) (7c_1^2 + c_2 c_3) \right\} \right] G_3 \left. \right\}, \tag{A11}
\end{aligned}$$

$$\begin{aligned}
A_6 = & [8\{-(m_\Lambda s + m_p c_\Lambda) \pm m_{N^*} (c_\Lambda + m_p m_\Lambda)\} c_1 (7c_1^2 + 3c_2 c_3)] G_1 \\
& + \frac{1}{2} \left[\left\{ -(m_p c_\Lambda - m_\Lambda c_p) \pm m_{N^*} \left(m_p m_\Lambda - \frac{1}{s} c_\Lambda c_p \right) \right\} \left\{ c_1 (7c_1^2 + 3c_2 c_3) + 3(7c_1^2 + c_2 c_3) (c_1 + b_p c_s) - \frac{6}{s} c_1 c_2 c_4 c_p \right\} \right. \\
& + b_p \left(-m_\Lambda \pm \frac{1}{s} m_{N^*} c_\Lambda \right) c_1 (7c_1^2 + 3c_2 c_3) \pm m_{N^*} \left\{ 21c_1 (3c_1^2 + c_2 c_3) (c_1 + b_p c_s) - \frac{3}{s} c_2 c_4 c_p (7c_1^2 + c_2 c_3) \right\} \left. \right] G_2 \\
& + \frac{1}{2} m_p \left[(-s \pm m_{N^*} m_p) \left\{ 21c_1 (3c_1^2 + c_2 c_3) c_s - 3c_2 (7c_1^2 + c_2 c_3) \left(1 + \frac{1}{s} c_p \right) \right\} \right. \\
& - c_1 (7c_1^2 + 3c_2 c_3) \left\{ (m_p m_\Lambda - 7c_\Lambda) \mp m_{N^*} \left(\frac{1}{s} m_p c_\Lambda - 7m_\Lambda \right) \right\} \\
& \left. + \left\{ 3(7c_1^2 + c_2 c_3) c_s - 6c_1 c_2 \left(1 + \frac{1}{s} c_p \right) \right\} \left\{ (b_p c_\Lambda - m_p m_\Lambda c_k) \pm m_{N^*} \left(\frac{1}{s} m_p c_\Lambda c_k - m_\Lambda b_p \right) \right\} \right] G_3. \tag{A12}
\end{aligned}$$

APPENDIX B: EXTRACTED NUCLEON RESONANCE COUPLING CONSTANTS

In this appendix we list the extracted coupling constants of nucleon resonances used in our analysis and compare them with those of our previous study [1]. Note that not all resonances used in the present study were available in the previous one. Furthermore, for the sake of brevity we do not list the corresponding error bars.

TABLE IV. The extracted nucleon resonance coupling constants from fits to experimental data in the present and previous [1] works.

Coupling	$L_{2I,2J}$	J^P	Present	Previous
$G_{N(1440)}/4\pi$	P_{11}	$1/2^+$	-0.17	1.52
$G_{N(1520)}^{(1)}/4\pi$	D_{13}	$3/2^-$	0.30	-0.00
$G_{N(1520)}^{(2)}/4\pi$			-0.91	0.68
$G_{N(1520)}^{(3)}/4\pi$			0.29	0.07
$G_{N(1520)}^{(4)}/4\pi$			0.32	-0.32
$G_{N(1535)}/4\pi$	S_{11}	$1/2^-$	0.13	-0.15
$G_{N(1650)}/4\pi$	S_{11}	$1/2^-$	0.09	-0.04
$G_{N(1675)}^{(1)}/4\pi$	D_{15}	$5/2^-$	-2.12	0.01
$G_{N(1675)}^{(2)}/4\pi$			0.35	0.87
$G_{N(1675)}^{(3)}/4\pi$			-1.88	0.07
$G_{N(1675)}^{(4)}/4\pi$			-0.63	-0.01
$G_{N(1680)}^{(1)}/4\pi$	F_{15}	$5/2^+$	-0.21	2.74
$G_{N(1680)}^{(2)}/4\pi$			6.15	0.05
$G_{N(1680)}^{(3)}/4\pi$			-0.37	2.54
$G_{N(1680)}^{(4)}/4\pi$			-3.01	0.44
$G_{N(1700)}^{(1)}/4\pi$	D_{13}	$3/2^-$	-0.10	0.25
$G_{N(1700)}^{(2)}/4\pi$			-0.95	0.62
$G_{N(1700)}^{(3)}/4\pi$			-0.38	0.51
$G_{N(1700)}^{(4)}/4\pi$			0.43	-0.20
$G_{N(1710)}/4\pi$	P_{11}	$1/2^+$	0.29	-0.41
$G_{N(1720)}^{(1)}/4\pi$	P_{13}	$3/2^+$	0.03	0.28
$G_{N(1720)}^{(2)}/4\pi$			0.22	-0.36
$G_{N(1720)}^{(3)}/4\pi$			0.04	0.17
$G_{N(1720)}^{(4)}/4\pi$			0.08	-0.21
$G_{N(1860)}^{(1)}/4\pi$	F_{15}	$5/2^+$	0.90	-2.20
$G_{N(1860)}^{(2)}/4\pi$			1.11	-9.99
$G_{N(1860)}^{(3)}/4\pi$			1.23	-2.28
$G_{N(1860)}^{(4)}/4\pi$			0.48	3.12
$G_{N(1875)}^{(1)}/4\pi$	D_{13}	$3/2^-$	-0.18	-0.13
$G_{N(1875)}^{(2)}/4\pi$			-1.76	-0.09
$G_{N(1875)}^{(3)}/4\pi$			0.20	-0.54
$G_{N(1875)}^{(4)}/4\pi$			0.65	0.11
$G_{N(1880)}/4\pi$	P_{11}	$1/2^+$	-0.40	0.33
$G_{N(1895)}/4\pi$	S_{11}	$1/2^-$	-0.01	0.01
$G_{N(1900)}^{(1)}/4\pi$	P_{13}	$3/2^+$	0.23	0.02
$G_{N(1900)}^{(2)}/4\pi$			0.22	-0.21
$G_{N(1900)}^{(3)}/4\pi$			0.16	0.05

(Table continued)

TABLE IV. (Continued)

Coupling	$L_{2I,2J}$	J^P	Present	Previous
$G_{N(1900)}^{(4)}/4\pi$			-0.29	0.38
$G_{N(1990)}^{(1)}/4\pi$	F_{17}	$7/2^+$	4.53	...
$G_{N(1990)}^{(2)}/4\pi$			1.67	...
$G_{N(1990)}^{(3)}/4\pi$			3.71	...
$G_{N(1990)}^{(4)}/4\pi$			-1.19	...
$G_{N(2000)}^{(1)}/4\pi$	F_{15}	$5/2^+$	-0.76	-1.44
$G_{N(2000)}^{(2)}/4\pi$			-10.0	9.75
$G_{N(2000)}^{(3)}/4\pi$			-1.57	0.33
$G_{N(2000)}^{(4)}/4\pi$			4.41	-4.13
$G_{N(2060)}^{(1)}/4\pi$	D_{15}	$5/2^-$	3.56	-0.69
$G_{N(2060)}^{(2)}/4\pi$			-2.57	0.82
$G_{N(2060)}^{(3)}/4\pi$			3.18	-0.91
$G_{N(2060)}^{(4)}/4\pi$			2.73	-1.51
$G_{N(2120)}^{(1)}/4\pi$	D_{13}	$3/2^-$	-0.05	0.05
$G_{N(2120)}^{(2)}/4\pi$			1.53	1.40
$G_{N(2120)}^{(3)}/4\pi$			0.09	0.06
$G_{N(2120)}^{(4)}/4\pi$			-0.62	-0.57
$G_{N(2190)}^{(1)}/4\pi$	G_{17}	$7/2^-$	-1.28	...
$G_{N(2190)}^{(2)}/4\pi$			6.08	...
$G_{N(2190)}^{(3)}/4\pi$			3.16	...
$G_{N(2190)}^{(4)}/4\pi$			-5.05	...
$G_{N(2220)}^{(1)}/4\pi$	H_{19}	$9/2^+$	-1.55	...
$G_{N(2220)}^{(2)}/4\pi$			10.0	...
$G_{N(2220)}^{(3)}/4\pi$			-10.0	...
$G_{N(2220)}^{(4)}/4\pi$			10.0	...
$G_{N(2250)}^{(1)}/4\pi$	G_{19}	$9/2^-$	-10.0	...
$G_{N(2250)}^{(2)}/4\pi$			-10.0	...
$G_{N(2250)}^{(3)}/4\pi$			-8.38	...
$G_{N(2250)}^{(4)}/4\pi$			-0.40	...

APPENDIX C: ELECTROMAGNETIC AND HADRONIC DECAY AMPLITUDES

To calculate the relative decay widths listed in Table III, we used Eqs. (48) and (49) which compute the radiative and hadronic decay widths, respectively. The former requires information on the helicity amplitudes $A_{1/2}$ and $A_{3/2}$, whereas the latter needs the hadronic decay amplitude $A_{K^+\Lambda}$. The helicity amplitudes can be related to the electromagnetic coupling constants g_1, \dots, g_4 by using the

electromagnetic interaction Lagrangian given by Eq. (10). To this end we follow the prescription given in Ref. [24]. The hadronic decay amplitude required for the calculation of the decay width given by Eq. (49) can be obtained by using the same prescription.

The electromagnetic and hadronic decay amplitudes for spin-3/2 resonances read

$$A_{1/2} = \frac{e}{4m_{N^*}^3} \sqrt{\frac{m_{N^*}^2 - m_N^2}{3m_N}} [-2ig_1 m_{N^*} (m_{N^*} \pm m_N) + g_2 m_{N^*} (m_{N^*} \mp m_N) - 2ig_3 (m_{N^*}^2 + m_N^2 \pm m_{N^*} m_N) + 2g_4 (m_{N^*}^2 + m_N^2 \mp m_{N^*} m_N)], \quad (C1)$$

$$A_{3/2} = \mp \frac{e}{4m_{N^*}^2} \sqrt{\frac{m_{N^*}^2 - m_N^2}{m_N}} [2ig_1 (m_{N^*} \pm m_N) + g_2 (m_{N^*} \mp m_N) + 2ig_3 (m_{N^*} \pm 2m_N) + 2g_4 (m_{N^*} \mp 2m_N)], \quad (C2)$$

$$A_{K^+\Lambda} = \pm i \frac{g_{K^+\Lambda N^*}}{m_{N^*}} \sqrt{\frac{E_\Lambda \mp m_\Lambda}{3m_\Lambda}} (E_\Lambda \pm m_\Lambda). \quad (C3)$$

For spin-5/2 resonances the electromagnetic and hadronic decay amplitudes are

$$A_{1/2} = \pm \frac{e}{8m_{N^*}^5} \sqrt{\frac{m_{N^*}^2 - m_N^2}{5m_N}} (m_{N^*}^2 - m_N^2) [-2ig_1 m_{N^*} (m_{N^*} \mp m_N) + g_2 m_{N^*} (m_{N^*} \pm m_N) - 2ig_3 (m_{N^*}^2 + m_N^2 \mp m_{N^*} m_N) + 2g_4 (m_{N^*}^2 + m_N^2 \pm m_{N^*} m_N)], \quad (C4)$$

$$A_{3/2} = \frac{e}{4m_{N^*}^4} \sqrt{\frac{m_{N^*}^2 - m_N^2}{10m_N}} (m_{N^*}^2 - m_N^2) [2ig_1 (m_{N^*} \mp m_N) + g_2 (m_{N^*} \pm m_N) + 2ig_3 (m_{N^*} \mp 2m_N) + 2g_4 (m_{N^*} \pm 2m_N)], \quad (C5)$$

$$A_{K^+\Lambda} = -i \frac{g_{K^+\Lambda N^*}}{m_{N^*}^2} \sqrt{\frac{E_\Lambda \mp m_\Lambda}{5m_\Lambda}} (E_\Lambda^2 - m_\Lambda^2), \quad (C6)$$

whereas for the spin-7/2 nucleon resonances the electromagnetic and hadronic decay amplitudes read

$$A_{1/2} = \frac{e}{8m_{N^*}^7} \sqrt{\frac{m_{N^*}^2 - m_N^2}{35m_N}} (m_{N^*}^2 - m_N^2)^2 [-2ig_1 m_{N^*} (m_{N^*} \pm m_N) + g_2 m_{N^*} (m_{N^*} \mp m_N) - 2ig_3 (m_{N^*}^2 + m_N^2 \pm m_{N^*} m_N) + 2g_4 (m_{N^*}^2 + m_N^2 \mp m_{N^*} m_N)], \quad (C7)$$

$$A_{3/2} = \mp \frac{e}{8m_{N^*}^6} \sqrt{\frac{m_{N^*}^2 - m_N^2}{21m_N}} (m_{N^*}^2 - m_N^2)^2 [2ig_1 (m_{N^*} \pm m_N) + g_2 (m_{N^*} \mp m_N) + 2ig_3 (m_{N^*} \pm 2m_N) + 2g_4 (m_{N^*} \mp 2m_N)], \quad (C8)$$

$$A_{K^+\Lambda} = \pm i \frac{g_{K^+\Lambda N^*}}{m_{N^*}^3} \sqrt{\frac{4(E_\Lambda \mp m_\Lambda)}{35m_\Lambda}} (E_\Lambda \pm m_\Lambda) (E_\Lambda^2 - m_\Lambda^2). \quad (C9)$$

Finally, the electromagnetic and hadronic decay amplitudes for spin-9/2 resonances are given by

$$A_{1/2} = \pm \frac{e}{16m_{N^*}^9} \sqrt{\frac{m_{N^*}^2 - m_N^2}{63m_N}} (m_{N^*}^2 - m_N^2)^3 [-2ig_1 m_{N^*} (m_{N^*} \mp m_N) + g_2 m_{N^*} (m_{N^*} \pm m_N) - 2ig_3 (m_{N^*}^2 + m_N^2 \mp m_{N^*} m_N) + 2g_4 (m_{N^*}^2 + m_N^2 \pm m_{N^*} m_N)], \quad (C10)$$

$$A_{3/2} = \frac{e}{16m_{N^*}^8} \sqrt{\frac{m_{N^*}^2 - m_N^2}{42m_N}} (m_{N^*}^2 - m_N^2)^3 [2ig_1 (m_{N^*} \mp m_N) + g_2 (m_{N^*} \pm m_N) + 2ig_3 (m_{N^*} \mp 2m_N) + 2g_4 (m_{N^*} \pm 2m_N)], \quad (C11)$$

$$A_{K^+\Lambda} = -i \frac{g_{K^+\Lambda N^*}}{m_{N^*}^4} \sqrt{\frac{4(E_\Lambda \mp m_\Lambda)}{63m_\Lambda}} (E_\Lambda^2 - m_\Lambda^2)^2. \quad (C12)$$

APPENDIX D: EXTRACTED MASSES AND WIDTHS OF NUCLEON RESONANCES

In this appendix we list the masses and widths of nucleon resonances used in our analysis. We also compare them with those obtained from the Review of Particle Properties of PDG [2]. For the sake of brevity we omit the error bars of the fitted masses or widths.

TABLE V. The masses (M) and widths (Γ) of the resonances used, obtained from PDG [2], and present work (PW). In the case that no error bars are provided by PDG, we add ± 100 MeV error bars.

Resonance	M (MeV)		Γ (MeV)	
	PDG	PW	PDG	PW
$N(1440)$	1430 ± 20	1420	350 ± 100	200
$N(1520)$	1515 ± 5	1515	115^{+10}_{-15}	100
$N(1535)$	1535 ± 10	1541	150 ± 25	125
$N(1650)$	1655^{+15}_{-10}	1670	140 ± 30	147
$N(1675)$	1675 ± 5	1680	150^{+15}_{-20}	130
$N(1680)$	1685 ± 5	1680	130 ± 10	140
$N(1700)$	1700 ± 50	1693	150 ± 100	106
$N(1710)$	1710 ± 30	1740	100^{+150}_{-50}	196
$N(1720)$	1720^{+30}_{-20}	1700	250^{+150}_{-100}	211
$N(1860)$	1860^{+100}_{-40}	1960	270^{+140}_{-50}	220
$N(1875)$	1875^{+45}_{-55}	1890	250 ± 70	306
$N(1880)$	1870 ± 35	1905	235 ± 65	300
$N(1895)$	1895 ± 15	1910	90^{+30}_{-15}	120
$N(1900)$	1900 ± 30	1885	200 ± 50	300
$N(2050)$	2050 ± 100	2150	460 ± 100	410
$N(2060)$	2060 ± 100	2005	375 ± 25	350
$N(2120)$	2120 ± 100	2052	330 ± 45	285
$N(1990)$	2060 ± 100	2110	240 ± 50	190
$N(2190)$	2190^{+10}_{-90}	2200	500 ± 200	300
$N(2220)$	2250 ± 50	2300	400^{+100}_{-50}	350
$N(2250)$	2275 ± 75	2200	500^{+300}_{-270}	800

- [1] T. Mart, S. Clymton, and A. J. Arifi, *Phys. Rev. D* **92**, 094019 (2015).
- [2] K. A. Olive *et al.* (Particle Data Group Collaboration), *Chin. Phys. C* **38**, 090001 (2014).
- [3] R. A. Adelseck, C. Bennhold, and L. E. Wright, *Phys. Rev. C* **32**, 1681 (1985).
- [4] J.-C. David, C. Fayard, G. H. Lamot, and B. Saghai, *Phys. Rev. C* **53**, 2613 (1996).
- [5] V. Pascalutsa and R. Timmermans, *Phys. Rev. C* **60**, 042201 (1999).
- [6] T. Mart and A. Sulaksono, *Phys. Rev. C* **74**, 055203 (2006).
- [7] T. Vranx, L. De Cruz, J. Ryckebusch, and P. Vancraeyveld, *Phys. Rev. C* **84**, 045201 (2011).
- [8] V. Shklyar, H. Lenske, and U. Mosel, *Phys. Rev. C* **82**, 015203 (2010).
- [9] F. A. Berends, J. W. van Holten, P. Nieuwenhuizen, and B. de Wit, *Nucl. Phys.* **B154**, 261 (1979).
- [10] V. Pascalutsa, *Phys. Lett. B* **503**, 85 (2001).
- [11] V. Pascalutsa, *Phys. Rev. D* **58**, 096002 (1998).
- [12] S. Z. Huang, P. F. Zhang, T. N. Ruan, Y. C. Zhu, and Z. P. Zheng, *Commun. Theor. Phys.* **41**, 405 (2004).
- [13] B. B. Deo and A. K. Bisoi, *Phys. Rev. D* **9**, 288 (1974).
- [14] P. Dennery, *Phys. Rev.* **124**, 2000 (1961).
- [15] F. James and M. Roos, *Comput. Phys. Commun.* **10**, 343 (1975).
- [16] T. Mart and A. K. Sari, *Mod. Phys. Lett. A* **28**, 1350054 (2013); L. Syukurilla and T. Mart, *Int. J. Mod. Phys. E* **24**, 1550008 (2015); *AIP Conf. Proc.* **1617**, 126 (2014).
- [17] T. Mart and C. Bennhold, *Phys. Rev. C* **61**, 012201 (1999).

- [18] T. Mart and N. Nurhadiansyah, *Few-Body Syst.* **54**, 1729 (2013).
- [19] T. Mart, *Phys. Rev. C* **87**, 042201(R) (2013).
- [20] R. L. Workman, L. Tiator, and A. Sarantsev, *Phys. Rev. C* **87**, 068201 (2013).
- [21] C. Patrignani *et al.* (Particle Data Group Collaboration), *Chin. Phys. C* **40**, 100001 (2016) and 2017 update.
- [22] T. Mart, *Phys. Rev. C* **62**, 038201 (2000).
- [23] S. Capstick and W. Roberts, *Phys. Rev. D* **49**, 4570 (1994); **58**, 074011 (1998).
- [24] G. Penner, Diploma thesis, Universität Giessen, 1997 (unpublished).
- [25] T. Feuster and U. Mosel, *Phys. Rev. C* **59**, 460 (1999).
- [26] T. Mart and M. J. Kholili, *Phys. Rev. C* **86**, 022201(R) (2012).
- [27] R. Bradford *et al.* (CLAS Collaboration), *Phys. Rev. C* **73**, 035202 (2006).
- [28] M. E. McCracken *et al.* (CLAS Collaboration), *Phys. Rev. C* **81**, 025201 (2010).
- [29] P. Bydžovský and T. Mart, *Phys. Rev. C* **76**, 065202 (2007); T. Mart, L. Tiator, D. Drechsel, and C. Bennhold, *Nucl. Phys.* **A640**, 235 (1998); H. Yamamura, K. Miyagawa, T. Mart, C. Bennhold, W. Glöckle, and H. Haberzettl, *Phys. Rev. C* **61**, 014001 (1999); A. Salam, K. Miyagawa, T. Mart, C. Bennhold, and W. Glöckle, *Phys. Rev. C* **74**, 044004 (2006).
- [30] M. Sumihama *et al.* (LEPS Collaboration), *Phys. Rev. C* **73**, 035214 (2006).
- [31] T. C. Jude *et al.* (Crystal Ball at MAMI Collaboration), *Phys. Lett. B* **735**, 112 (2014).
- [32] T. Mart, *Phys. Rev. D* **83**, 094015 (2011); AIP Conf. Proc. **1454**, 19 (2012); *Phys. Rev. D* **88**, 057501 (2013); Proc. Sci., Hadron2013 (2013) 144; *Few-Body Syst.* **54**, 311 (2013).
- [33] A. Lleres *et al.* (GRAAL Collaboration), *Eur. Phys. J. A* **31**, 79 (2007).
- [34] R. Schumacher, in *Proceedings of the 9th International Conference on Hypernuclear and Strange Particle Physics (HYP 2006), Mainz, Germany, 2006*, edited by J. Pochodzalla and T. Walcher (University of Mainz, Mainz, Germany, 2007), p. 339.
- [35] A. Lleres *et al.* (GRAAL Collaboration), *Eur. Phys. J. A* **39**, 149 (2009).
- [36] R. Bradford *et al.*, *Phys. Rev. C* **75**, 035205 (2007).